Ltr. No. 78F-0720-143

STO / Dr. Pike

File: Union Carbide : misc.

31 AUG 1978

1

UNION CARBIDE CORPORATION
NUCLEAR DIVISION
P. O. BOX Y, OAK RIDGE, TENNESSEE 37830

July 20, 1978

SLL 80-190/M

Air Force Weapons Laboratory
Attention: Capt. N. Pchelkin
Chemical Laser Branch
Kirtland Air Force Base, New Mexico 87115

Department of Defense
Defense Advanced Research Projects Agency
Attention: Capt. H. Winsor
Materials Science Section
1400 Wilson Blvd
Arlington, Virginia 22209

Gentlemen:

Advanced Low-Heat-Loss Nozzle Research Program

The work conducted during the period February 15, 1978 to June 12, 1978, on AFWL Project Order 78-002, is presented in the enclosed report. This work covers the completion of the thermocouple experiments, the testing of materials in the configuration testing assembly, and the continued testing of cylindrical specimens involving old and new materials.

Please direct any comments you might have regarding this report to Mr. Z. L. Ardary.

Very truly yours,

W. H. Dodson, Director
Development Division

LK:tf

Attachment: Y/DA-7932

Distribution: Same as listed in report

19980309 386

Report Number Y/DA-7932

MATERIALS FOR HIGH-TEMPERATURE HYDROGEN-FLUORINE ENVIRONMENTS

AFWL Project Order 77-054

C. E. Holcombe
L. Kovach

DISTRIBUTION STATEMENT A
Approved for public release;
Distribution Unlimited

UNION CARBIDE

NUCLEAR DIVISION - GENERAL STAFF
OAK RIDGE, TENNESSEE

prepared for the U.S. DEPARTMENT OF ENERGY *under*
U.S. GOVERNMENT *Contract W-7405 eng 26*

DTIC QUALITY INSPECTED 4

PLEASE RETURN TO:

BMD TECHNICAL INFORMATION CENTER
BALLISTIC MISSILE DEFENSE ORGANIZATION
7100 DEFENSE PENTAGON
WASHINGTON D.C. 20301-7100

U3954

ENDORSEMENT NOTICE

Reference to a company or product name does not imply approval or recommendation of the product by Union Carbide Corporation or the Department of Energy to the exclusion of others that may meet specifications.

This report was prepared as an account of work sponsored by an agency of the United States Government. Neither the United States Government nor any agency thereof, nor any of their employees, nor any of their contractors, subcontractors, or their employees, makes any warranty, express or implied, nor assumes any legal liability or responsibility for any third party's use or the results of such use of any information, apparatus, product or process disclosed in this report, nor represents that its use by such third party would not infringe privately owned rights.

Accession Number: 3954

Publication Date: Jul 03, 1978

Title: Materials for High-temperature Hydrogen-Fluorine Environments

Personal Author: Holcombe, C.E.; Kovach, L.

Corporate Author Or Publisher: Union Carbide Corporaton, Nuclear Division, PO Box Y, Oak Ridge, TN 37 Report Number: Y/DA-7932 Report Number Assigned by Contract Monitor: SLL 80-190

Comments on Document: Archive, RRI, DEW.

Descriptors, Keywords: Material High Temperature Hydrogen Fluorine Environment Test Cylinder Embed Thermocouple Graphite Lanthanum Hexaboride Magnesia Nickel Aluminide Property Machine Plasma Spray Solid Solution Thermal Analysi

Pages: 00055

Cataloged Date: Nov 30, 1990

Document Type: HC

Number of Copies In Library: 000001

Record ID: 25346

Source of Document: DEW

Report Number Y/DA-7932

MATERIALS FOR HIGH-TEMPERATURE HYDROGEN-FLUORINE ENVIRONMENTS

AFWL Project Order 77-054

C. E. Holcombe
L. Kovach

July 3, 1978

OAK RIDGE Y-12 PLANT
P. O. Box Y, Oak Ridge, Tennessee 37830
Operated by
UNION CARBIDE CORPORATION, NUCLEAR DIVISION
for the
DEPARTMENT OF ENERGY, OAK RIDGE OPERATIONS

CONTENT

SUMMARY

This report is a continuation of the testing of candidate materials for use as uncooled nozzles for a hydrogen-fluorine laser system currently being developed by the Defense Advanced Research Projects Agency (DARPA), the Air Force Weapons Laboratory (AFWL), and the Missile Research and Development Command (MIRADCOM).

Thirty-three runs were completed in the HF test facility with materials of current interest to the project. Included were thermocouple experiments conducted with graphite, magnesia (MgO), nickel-270, nickel aluminide (NiAl), and lanthanum hexaboride (LaB_6) cylindrical specimens. With the exception of LaB_6, all specimens were tested to failure in order to determine the "break point" or surface temperature at which the protective film breaks down and rapid reaction starts. Temperature versus time curves are plotted for all specimens.

Test plates of graphite, MgO, alumina (Al_2O_3), and nickel-200 were tested in the materials test chamber and the resulting data agreed with the data for cylindrical test specimens. Little or no observable corrosion of the graphite test chamber body occurred.

Data were also collected from the testing of new materials, in the form of cylindrical specimens. Materials involved were dense calcium hexaboride (CaB_6), dense yttria (Y_2O_3), a lanthanum fluoride/tantalum (LaF_3/Ta) composite, a solid solution of lanthanum/strontium hexaboride ($La_{0.33}Sr_{0.67}B_6$) and substrates of nickel-270, POCO graphite, and W/Ni/Fe plasma-sprayed with LaB_6. "Break-point" temperatures were determined for CaB_6, Y_2O_3, and LaB_6. Plasma-sprayed LaB_6 shows promise of protecting substrate materials, particularly in the case of POCO graphite.

A ranking of the best fluoride film-formers with maximum-use temperature for near-zero corrosion in the 1800K-1400K range is:

$$LaB_6 > CaB_6 > La_2O_3 \cdot Si_3N_4 > (Sc, SrO, LaCrO_3, Ni)$$

INTRODUCTION

The HF (hydrogen-fluoride) chemical laser requires high-temperature, hydrogen-fluoride molecules that are excited to an elevated vibrational state and allowed rapid expansion.

The principal nozzle material previously considered was nickel—requiring internal cooling and thus special machining for coolant flow, as well as creating reduced lasing efficiencies from the high energy losses through the flowing coolant. Therefore, interest has developed in uncooled nozzle materials in the activity entitled "Advanced Low-Heat-Loss Nozzle Research Program."

Previous reports[1-3] described the design, construction, and operation of the HF facility and discussed the initial materials selection criteria. Included were results of the initial screening phase of the program, and the testing of 136 specimens, plus some physical property data. The upper use-temperatures for near-zero corrosion, as determined for 12 different materials, was also included.

Three types of materials testing experiments are covered in this report: (1) the continuation of material (old and new) evaluations using cylindrical specimens, (2) the testing of cylindrical specimens with embedded thermocouples, and (3) the testing of flat plates in the materials test chamber assembly.

SECTION I. TEST CYLINDERS WITH EMBEDDED THERMOCOUPLES

A. Experimental

In an effort to define true surface temperature, experiments were devised whereby thermocouples are inserted into the specimens undergoing test. The temperature-measuring techniques employed and the results obtained on runs conducted with alumina are described in previous reports.[2,3] Calculation of true specimen surface temperatures from the thermocouple data using thermal conduction equations and extrapolation techniques indicated both methods essentially gave the same results. Calculated surface temperatures differed from top center thermocouple readings by a maximum of 20°C, with an average difference of 10°C. Comparable temperature differences, employing extrapolation techniques, were obtained for the thermocouple experiments described in this report.

B. Results and Discussions

1. Graphite

Two runs, HF-139 and HF-144, were made with ATJ graphite specimens; time versus temperature data are plotted in Figure 1 for Run HF-144. In this run, the specimen heated up rapidly to a maximum of 1543K, and a "break-point" temperature, according to the top thermocouple reading, was 1138K. We were aware that the "break-point" temperature or surface temperature of emergence of rapid reaction for graphite was in the vicinity of the point at which the automatic pyrometer started to indicate, but this is the first instance in which the "break-point" temperature was clearly recorded. Automatic and manual radiation pyrometer readings are included in Figure 1 and these show a temperature about 40K higher than the top thermocouple reading in the temperature region of 1500K.

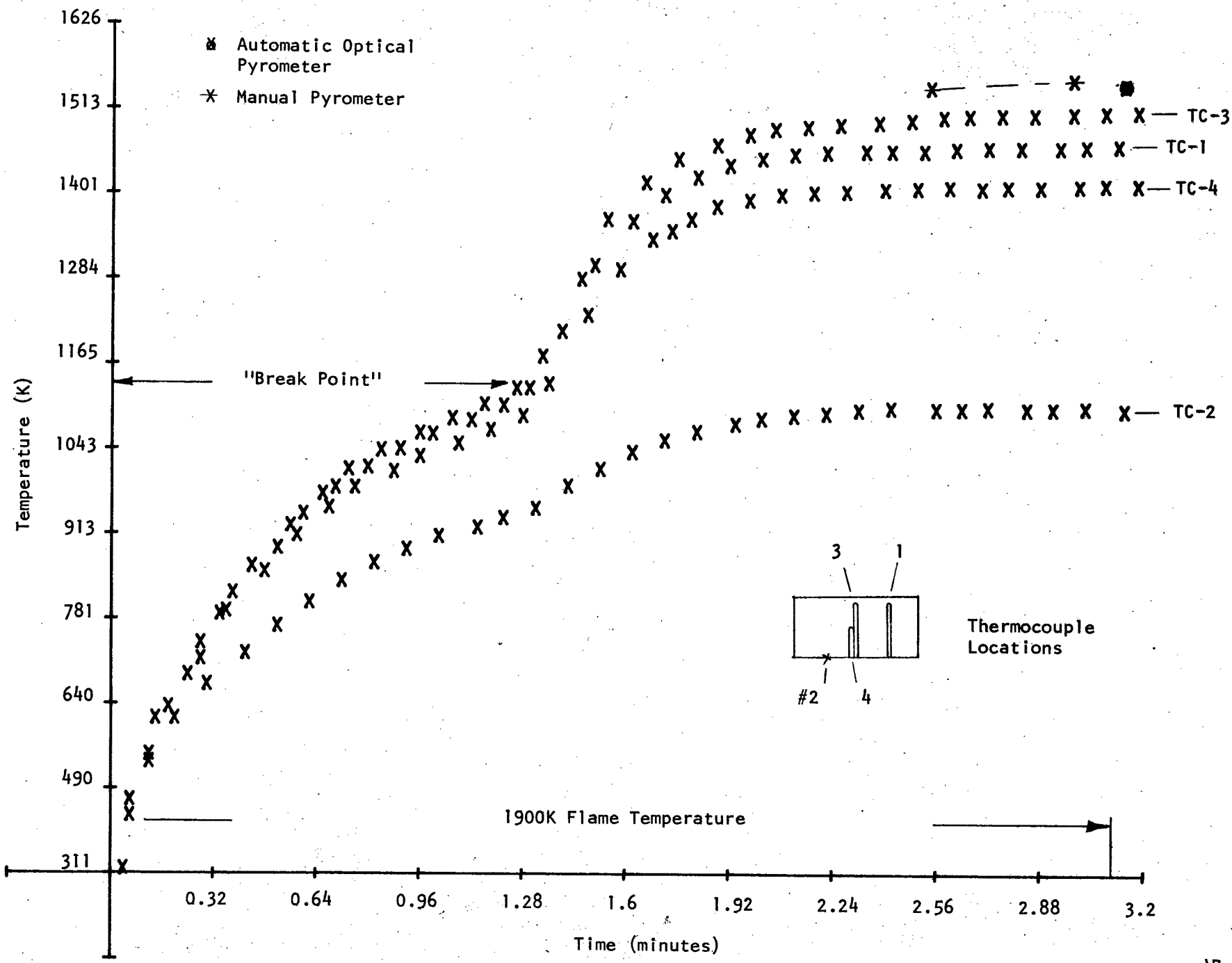

Figure 1. TEMPERATURE VERSUS TIME CURVE FOR ATJ GRAPHITE EXPOSED TO HF FLAME (Run HF-144).

2. Lanthanum Hexaboride

Two thermocouple experiments were conducted with a lanthanum hexaboride specimen. The specimen was mounted on alumina grit, in each instance, in order to reduce the amount of heat conducted away by the nickel specimen support. In Run HF-141, in which the highest flame temperature used was 2690K, a maximum specimen surface temperature of only 1571K was attained. The second run, HF-142, was made with the same specimen, but higher flame temperatures were employed. Figure 2 presents the temperature versus time data for Run HF-142. Employing flame temperatures to above 2853K, a maximum specimen surface temperature of 1720 K, as indicated by the automatic optical pyrometer, was reached. At this point, thermocouple readings became erratic, and, in fact, the No. 4 thermocouple inserted in the center of the specimen failed; the nickel thermocouple sheath had melted indicating that the temperature had reached the melting point of nickel, namely 1726K.

The temperature plot also shows a more than 70K difference between thermocouple and pyrometer readings, which is unlike the situation with the graphite samples. No explanation is offered at this time, other than that this larger temperature difference ties in with the thermal resistance and characteristics of the lanthanum fluoride layer.

The LaB_6 specimen used in the above tests was determined to have a bulk density of 4.68 g/cm^3 which is 99.3% of theoretical.

3. Magnesia (MgO)

Within a period of three minutes, during the first run (HF-138) conducted with MgO, the specimen split in two pieces in a plane running through the three drilled thermocouple holes. Indications were that stresses may have developed during the drilling operation.

For the second run, a single crystal MgO specimen was employed having only two thermocouple holes. After operating with a 1700K flame for 3.75 minutes and an 1830K flame for 1.5 minutes, the run was aborted because the flame was seen to be off-center. Upon adjustment of the nozzle, the run (HF-147) was continued with the same specimen, even though it had developed visible cracks. The run was terminated after 17.05 minutes, during which time it was observed that a portion of the specimen had melted and the center thermocouple hole became visible.

The temperature versus time data for Run HF-147 are plotted in Figure 3. The data indicate a "break point" occurred at around 1256K, after which there was a rapid temperature rise to 1421K (per automatic pyrometer scan). The pyrometer and top thermocouple readings differ by about 70K.

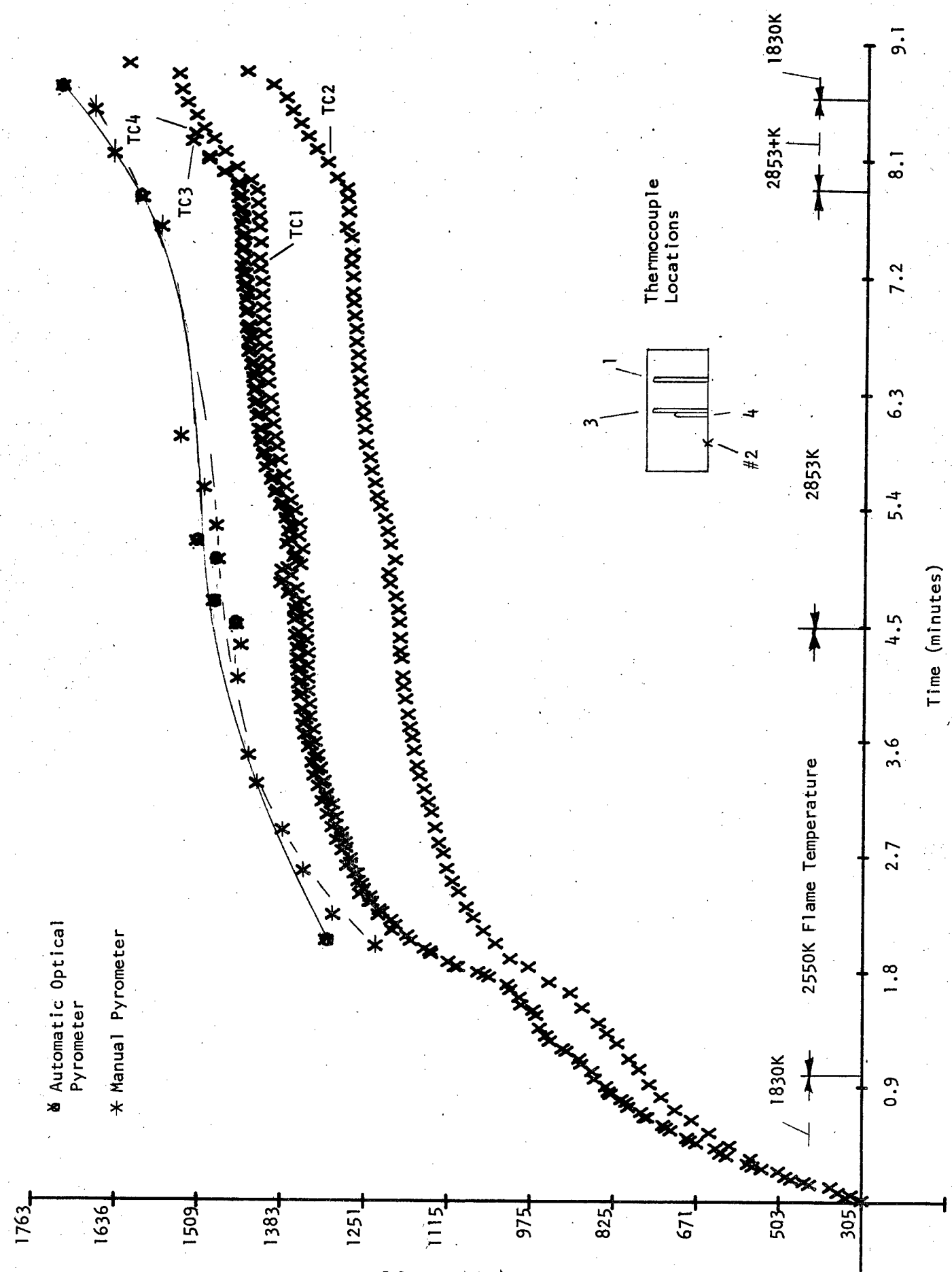

Figure 2. TEMPERATURE VERSUS TIME CURVE FOR LaB_6 EXPOSED TO HF FLAME (Run HF-142).

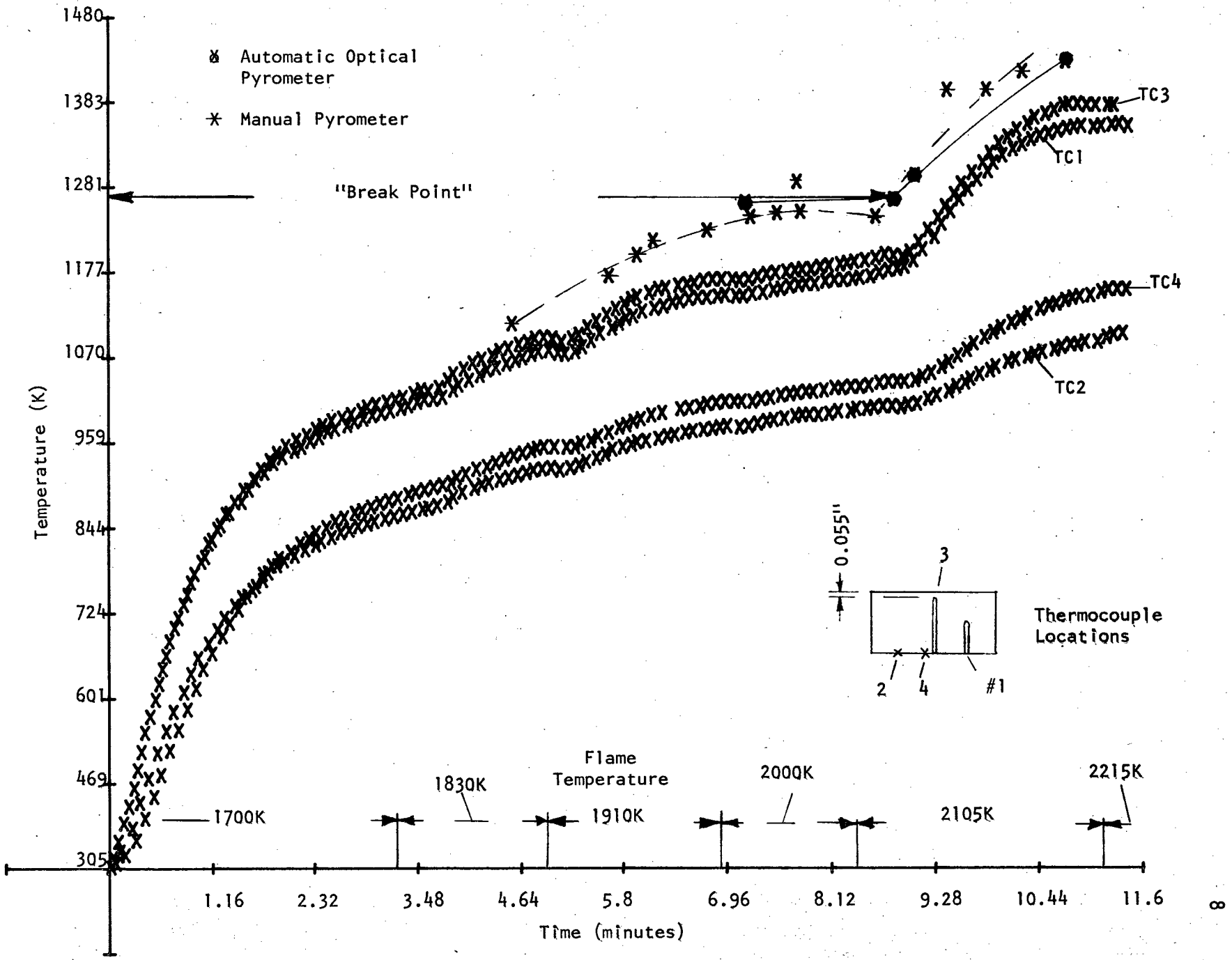

Figure 3. TEMPERATURE VERSUS TIME CURVE FOR MgO (SINGLE CRYSTAL) EXPOSED TO HF FLAME (Run HF-147).

The "break point" temperature 1256K determined above, compares favorably with data previously obtained on MgO; 1241K and 1248K.[3]

4. Nickel

Time versus temperature data on a nickel-270 specimen (Run HF-140) are plotted in Figure 4. With a flame temperature of 2395K, thermocouple readings rise rapidly to a maximum of 1698K, and the maximum automatic pyrometer reading attained was 1680K. The surface temperature of the nickel specimen was actually higher, since the specimen did melt, and the melting point of nickel is 1726K.

Nickel does have a "break point" temperature which is estimated to be 1425K. A previous experiment determined the maximum surface temperature for near-zero corrosion of nickel to be 1390K.[3]

5. Nickel Aluminide (NiAl)

Another of the metallic materials tested was NiAl, which is essentially an equimolecular compound of aluminum and nickel. Time versus temperature data on the NiAl specimen (Run HF-149), are presented in Figure 5. After about 2.5 minutes, there is a "break point", which according to the thermocouple readings is 1304K; the pyrometer recorder reading at the same time is 1380K. In previous work,[3] the zero-corrosion surface temperature for NiAl was reported to be 1390K.

The maximum thermocouple and pyrometer readings recorded are 1569K and 1646K, respectively. The nickel specimen support and the top center nickel thermocouple sheath became attached to the specimen during the run, indicating there was a reaction with the NiAl.

SECTION II. MATERIALS TEST CHAMBER ASSEMBLY

A. Experimental

An ATJ graphite cylindrical test chamber was fabricated for the purpose of evaluating the erosion effects as well as the chemical and temperature effects of the HF torch on candidate test materials. Design of the chamber was discussed in the previous report.[3]

Operation of the test chamber was satisfactory. The distance between the nozzle tip and test plate was maintained at 98.4 mm (3 7/8 in), and the gas flows employed were the same as those used for testing the 25.4-mm-diameter cylindrical specimens. The sapphire window in the chamber sightport permitted observation of the flame, the test plate, and scanning with the optical pyrometer. After six runs, no etching of the sapphire window was noted. Pressure buildup in the chamber, in the runs conducted thus far, did not exceed 2 psig. A nickel-sheathed

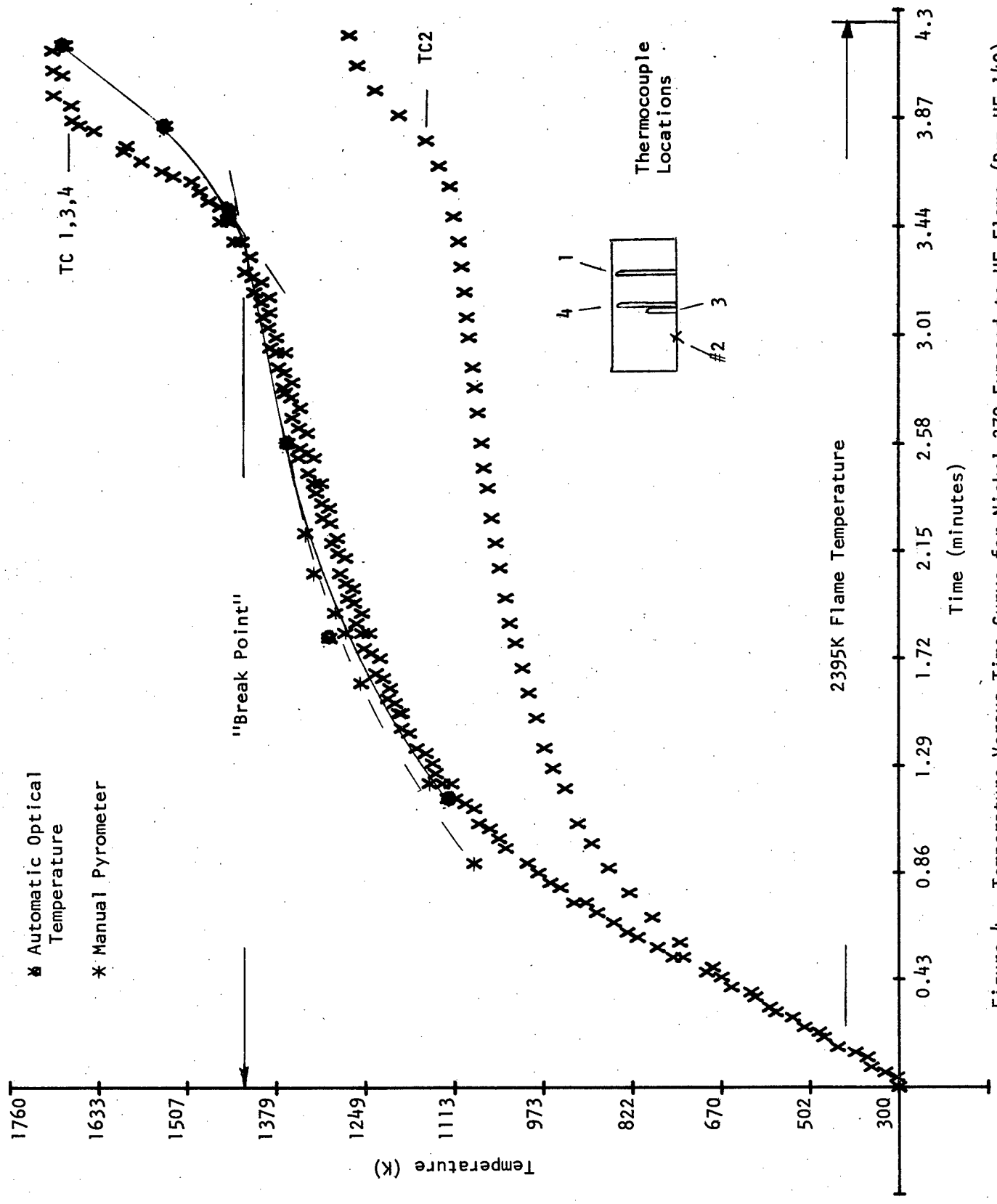

Figure 4. Temperature Versus Time Curve for Nickel-270 Exposed to HF Flame (Run HF-140).

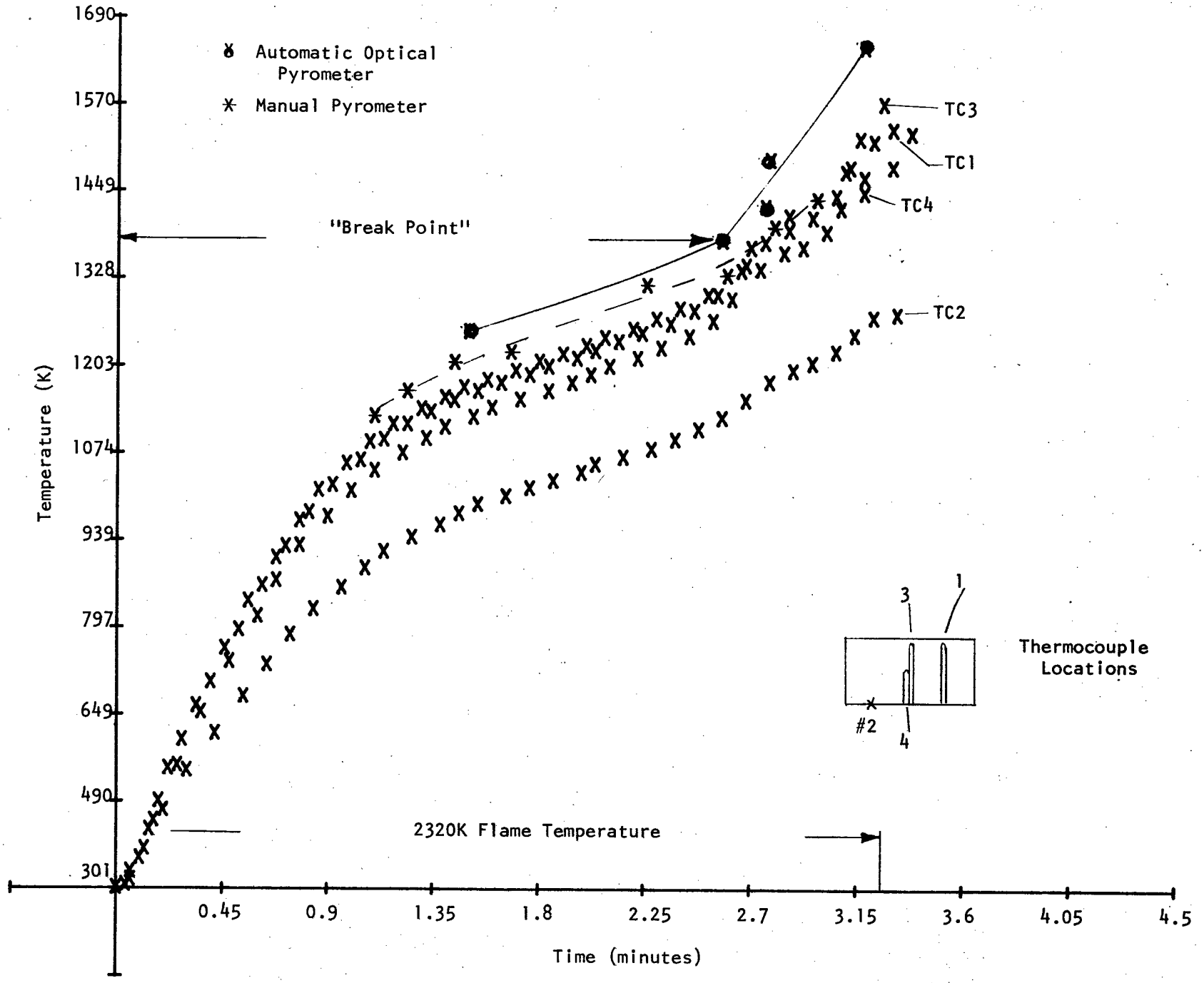

Figure 5. TEMPERATURE VERSUS TIME CURVE FOR NICKEL ALUMINIDE EXPOSED TO HF FLAME (Run HF-149).

thermocouple, fastened to the exterior bottom of the chamber, and positioned as close to the center of the plate as permissible, provided some of the temperature data. In tablulating the pyrometer data, in Appendix II, it was necessary to add another correction to the readings in order to compensate for the sapphire window in the test chamber sightport. This correction ranged from 6° to 17°C for readings between 800°C and 1600°C.

B. Results and Discussion of Test Plate Performance

1. ATJ Graphite

Initial runs in the test chamber were made with two ATJ graphite test plates, 3.81-mm thick, drilled with thirty-six 1.016-mm-diameter holes, set in a square array on 5.59 mm centers. In the first run, HF-145, a flame temperature of 1700K was employed. After 5.6 minutes, the run was terminated. At no time did the plate get hot enough to enable pyrometer readings to be taken. Data for this run and the following test chamber experiments are all presented in Appendices I and II.

In the second run, HF-146, the flame temperature was 1900K. After about 4.25 minutes, the test plate started to react, as evidenced by the rapid rise in both thermocouple and pyrometer temperature readings. The holes in the test plate were observed to increase in size, and the pressure in the test chamber dropped to 0 psig.

Figure 5 shows the condition of the test plates that were exposed to the HF flame during runs HF-145 and HF-146. For run HF-145, the test plate shows that the protective CF_x film was retained, and there was no evidence of corrosion. For run HF-146, the protective film in the center area with the holes is gone, and enlargement of the holes and corrosion in this area is evident. Figure 7 shows the faces of the plates that were directed away from the HF flame. One comment to be made in regard to plate HF-146 is that the temperature in the white outer ring area was lower (< 1138K) than the temperature in the center.

Examination of the test chamber assembly upon completion of both runs showed that the interior was still black and unaffected, and had, therefore, experienced no appreciable temperature rise.

Two additional ATJ graphite plates, 3.8-mm thick, were fabricated for testing in the chamber, but the openings in the plates were slots instead of holes. Each plate had 5 slots, 12.7-mm long, spaced 5.59 mm apart with tapered cross sections. Typically, as for run HF-156, the taper ranged from 1.016 to 1.067 mm wide on both sides of the plate down to 0.356-0.457 mm wide in the interior of the plate.

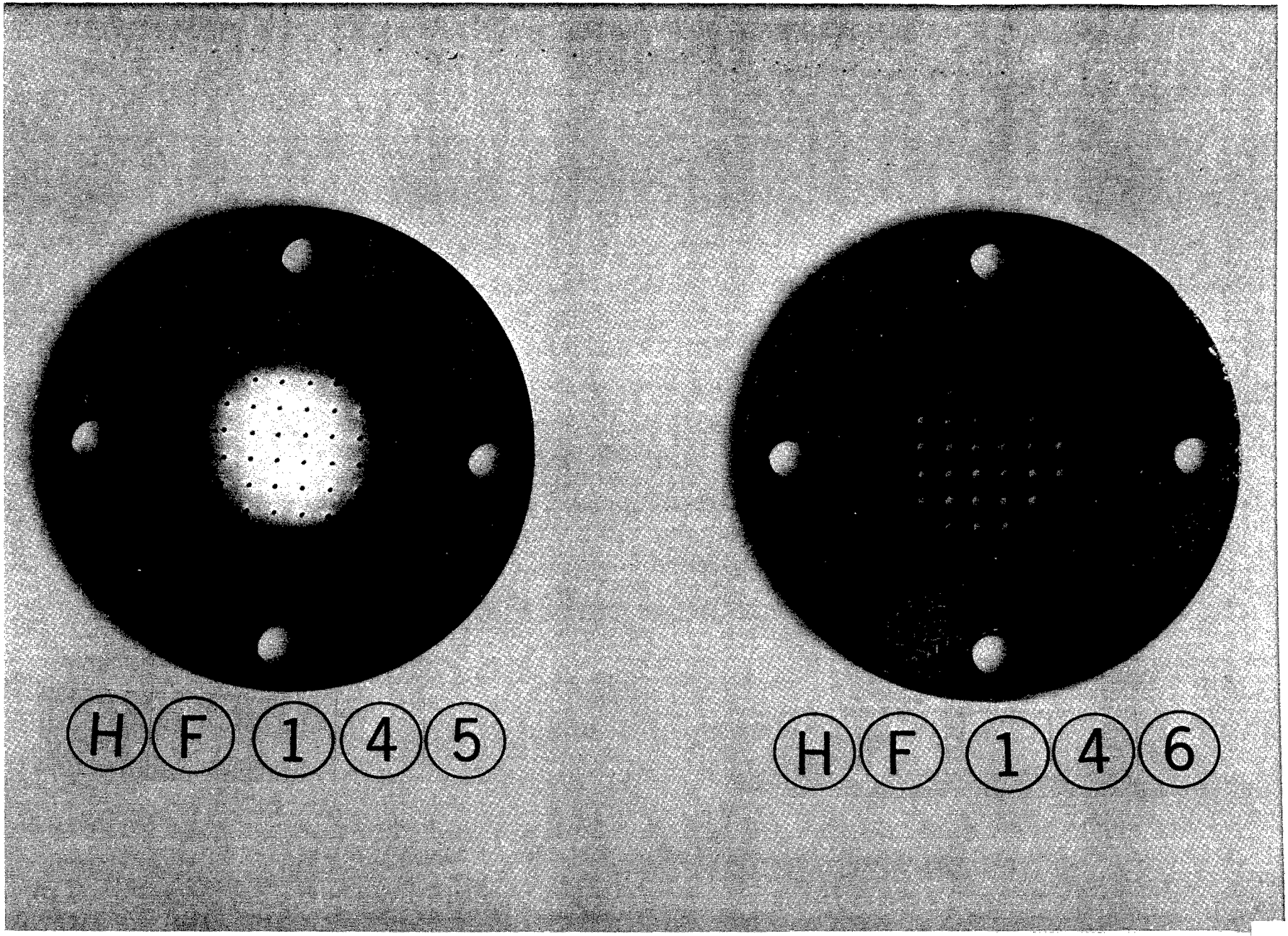

Figure 6. ATJ GRAPHITE TEST PLATES—FACES EXPOSED TO HF FLAME (Runs HF 145 & 146).

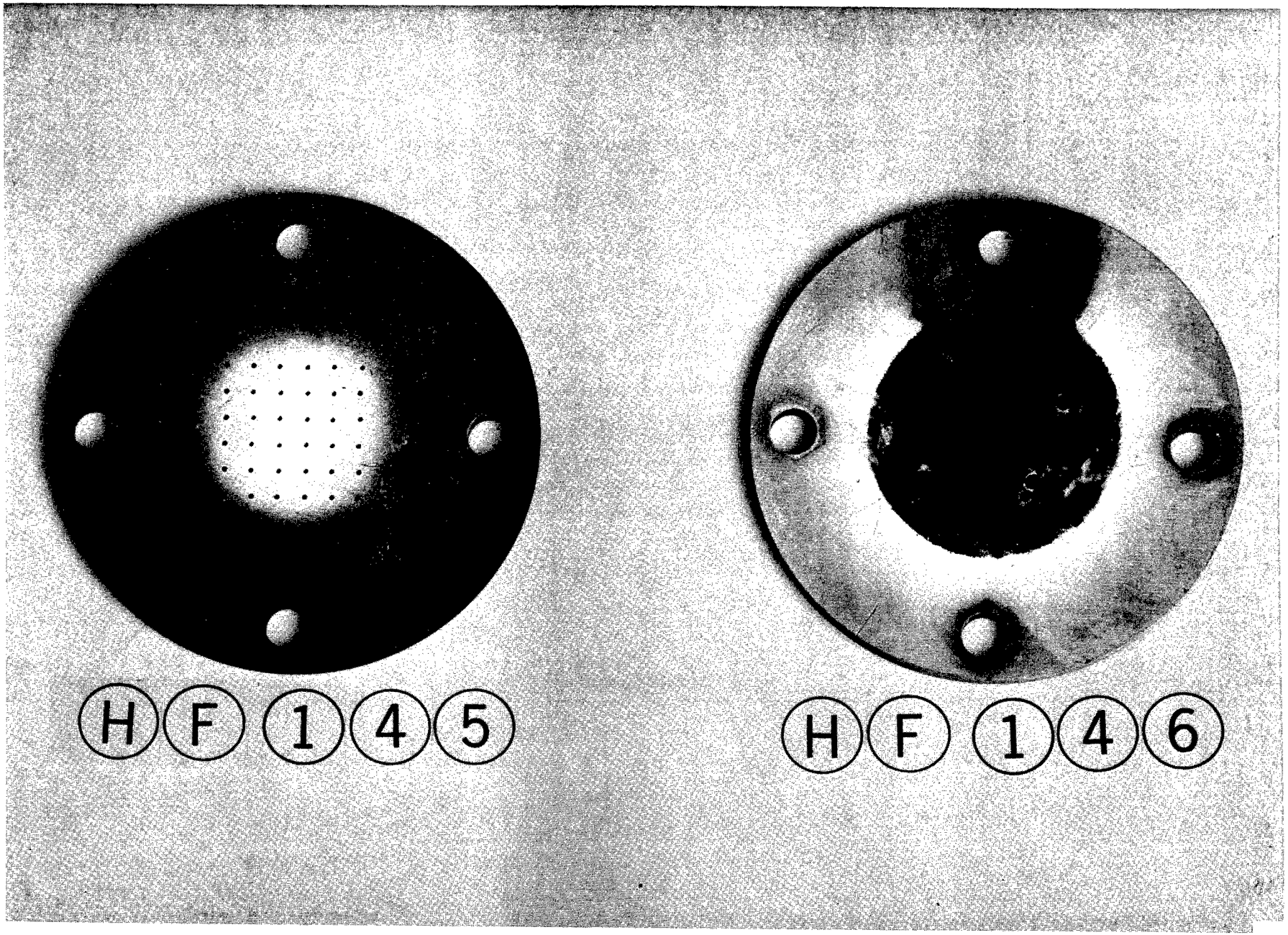

Figure 7. ATJ GRAPHITE TEST PLATES—EXTERIOR FACES (Runs HF 145 & 146).

HF-156 was conducted with a 1900K flame temperature. In the interval of 38 seconds, the graphite plate reacted and pyrometer readings rapidly increased to 1635K. Figure 8 shows the face of the plate (HF-156) that had been exposed to the HF flame. It is apparent that corrosion occurred in the immediate area of the slots and the slots had increased in cross section. A second run, HF-158, was conducted with a 1700K flame temperature. Here, too, the graphite plate reacted and temperatures increased rapidly; however, not until 4.33 minutes of the run had elapsed. In Figure 10, the exposed face of plate HF-158 is also exhibited. Again, the corrosive action is seen to have occurred in the area of the slots. The faces of plates HF-156 and HF-158, downstream from the HF flame, are shown in Figures 9 and 11.

Evidently there was a difference in behavior between the two sets of test plates; those with holes versus those with slots. This behavior, apparently, is explained by differences in configuration. The sharp, thin edges contained within the slots protrude into the hot-gas stream and heat up more rapidly to the temperature at which the protective film fails and corrosion begins.

2. Magnesia (MgO)

A MgO plate, having multiple holes and the same configuration as graphite plate HF-145, was fabricated and tested. During the experimental run (HF-155), in which a flame temperature of 1700K and 1830K was employed, the plate cracked into several pieces. The plate may have cracked at the beginning of the experiment since the chamber pressure was only approximately 1 psig. During the progress of the run, after 3.93 minutes, a "break point" temperature of 1247K was attained, as observed on the pyrometer recorder chart. Previous data on MgO specimens reported the surface temperature of emergence of rapid reaction to be 1241K and 1248K.[3]

The condition of the front and rear faces of the MgO plate after test in shown in Figures 8 and 9. Observation shows that the center area with the holes did experience some corrosion.

An additional observation was made that, in this instance, the interior of the graphite chamber had reacted with the HF torch gases since a higher flame temperature was required to test the MgO plate to the failure point.

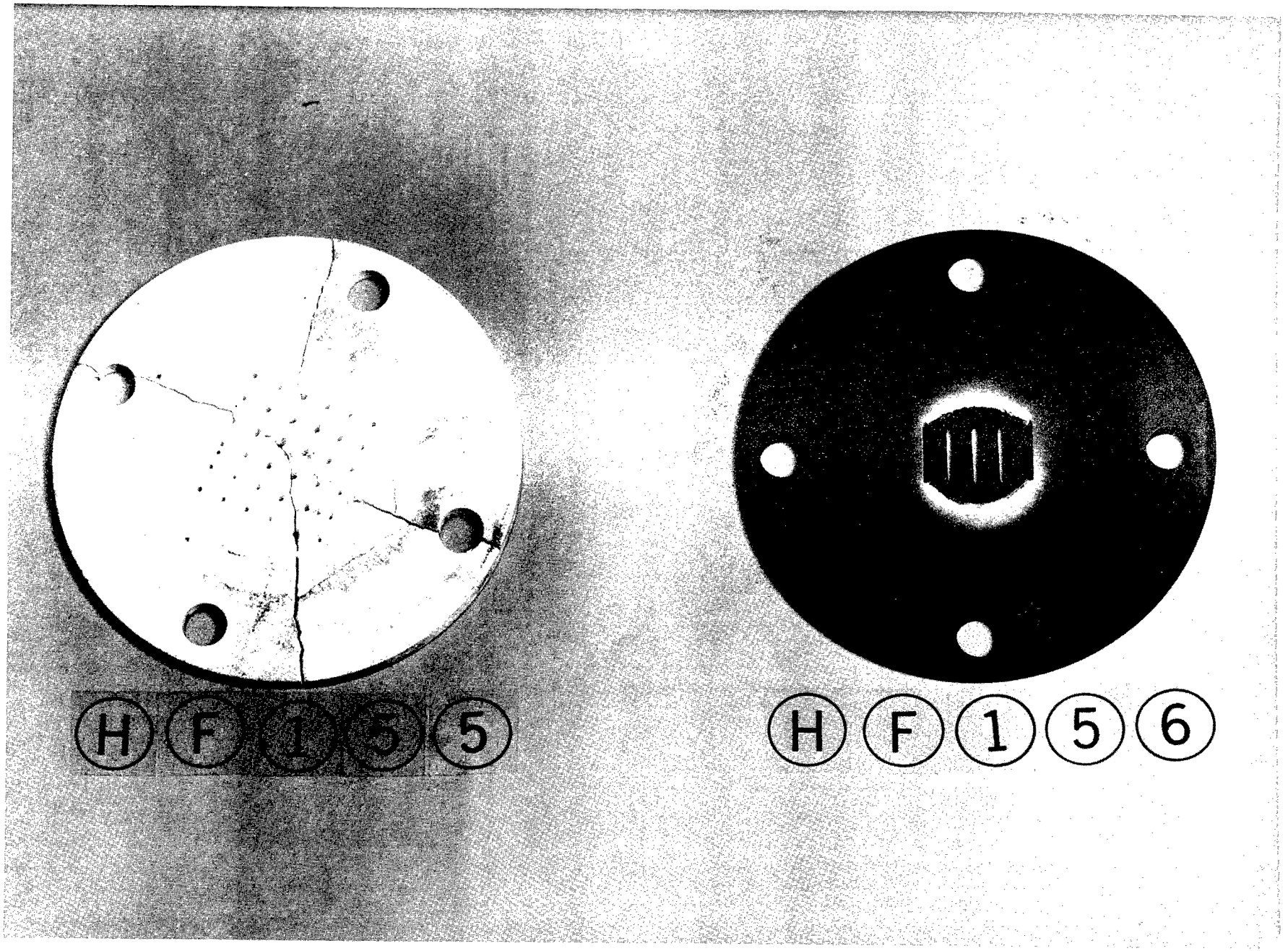

Figure 8. MgO (HF-155) and ATJ Graphite (HF-156) Test plates — Faces Exposed to HF Flame.

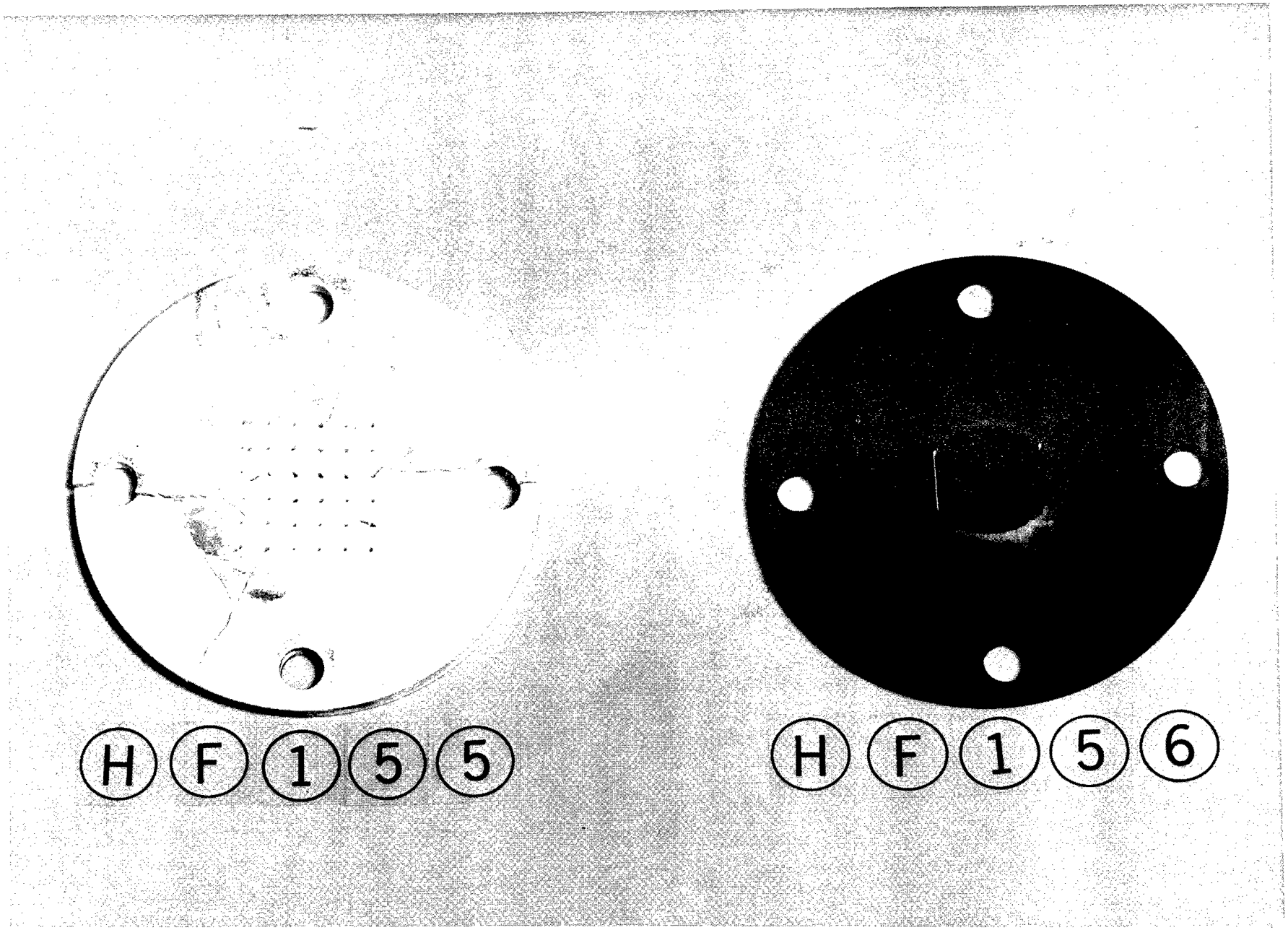

Figure 9. MgO (HF-155) and ATJ Graphite (HF-156) Test Plates — Outside Faces.

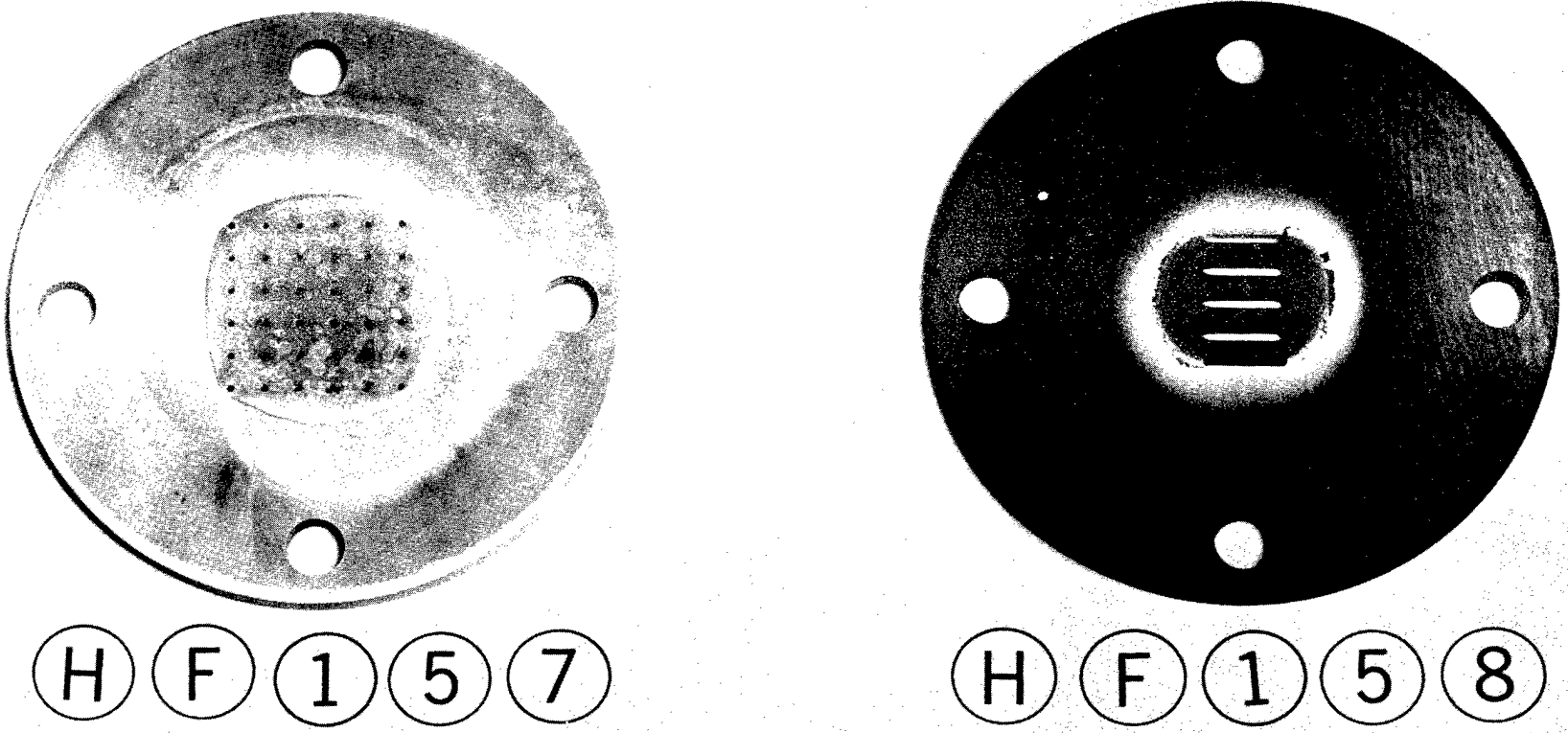

Figure 10. Nickel-100 (HF-157) and ATJ Graphite (HF-158) Test Plates — Faces Exposed to HF Flame.

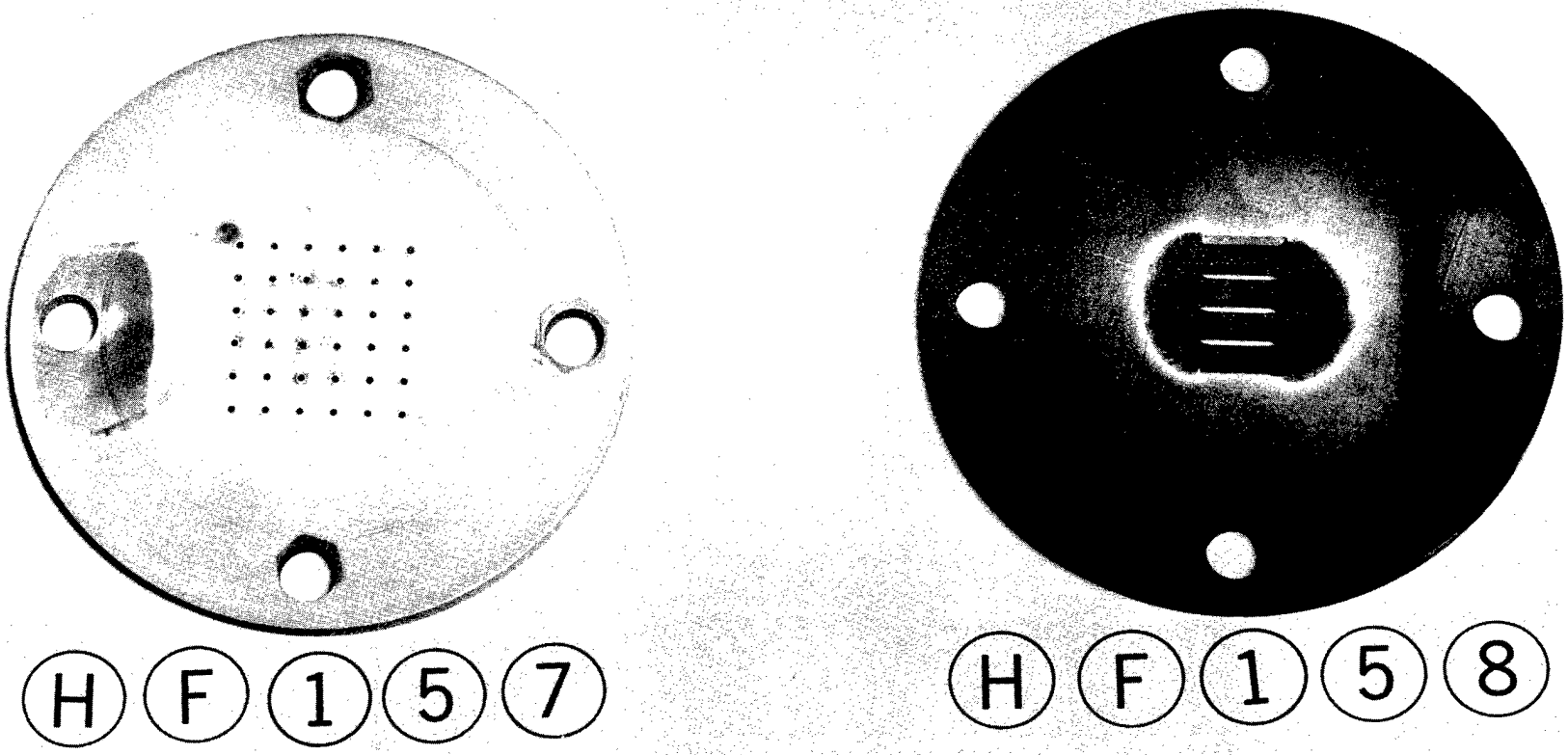

Figure 11. Nickel-200 (HF-157) and ATJ Graphite (HF-158) Test Plates — Outside Faces.

3. Alumina (Al_2O_3)

A run (HF-159) conducted with a test plate of alumina was not successful in that a section of the plate cracked and fell away; this was not evident until the run was finished. With a flame temperature of 1700K, the surface of the alumina reached a maximum temperature of 1416K as determined by the automatic pyrometer. No temperature "break points" were noted on either the pyrometer recorder or thermocouple recorder charts. Figure 12 shows the exposed side of the plate. The surface of the alumina does show evidence of corrosion.

4. Nickel-200

Another chamber experiment was conducted with a nickel-200 test plate having a 36-hole configuration similar to plate HF-145. In this run, HF-157, there was a steady rise in specimen surface temperature up to 1437K, at which time the run was terminated; no "break point" temperature was apparent. The front and rear faces of the tested plate are shown in Figures 10 and 11. The plate did experience a slight amount of corrosion, particularly in the center of the plate where the hole sizes were enlarged.

SECTION III. FURTHER MATERIALS EVALUATIONS

Since the previous report,[3] data for additional cylindrical specimens tested have been tabulated and are shown in Appendices I and II. It is apparent from Section I of this report that a fluoride film failure point or "break point", T_f can be determined from the temperature versus time profiles of the samples tested. Empirically, if the sample surface temperature is $\leq$ 95% of T_f (including emissivity corrections), near-zero corrosion occurs—or such a point represents a conservative maximum use-temperature.

A. Lanthanum Hexaboride (LaB_6)

Previous tests on lanthanum hexaboride (LaB_6) failed to cause a characteristic temperature rise from rapid exothermic reaction; a point where some flowing of the LaF_3 film occurs at 1636K (1756K with emissivity correction) was thought to represent failure—even though the fluoride was still highly viscous and protective. By thermally insulating the underside of a specimen with a porous LaF_3 layer, as in run HF-171, and by a slow, continual reduction of fluorine from the $2F_2/H_2$ ratio to $1.6F_2/H_2$ to increase the flame temperature above 2853K, a characteristic film failure was noted followed by rapid exothermic reaction, yielding the T_f of 1874K. The specimen lost $\sim$ 10% weight and had no LaF_3 film after testing. A possible explanation for the loss of LaF_3 between 1756K and 1874K is: (1) the viscosity of the LaF_3 becomes low enough to allow rapid flow, and (2) rapid vaporization of the LaF_3 occurs simultaneously. Thus, the reported LaF_3 melting point (1765K) may be exceeded by $\sim$ 100K before film failure, and then, the LaB_6 behaves as if its fluoride sublimes, thereby retaining its configuration.

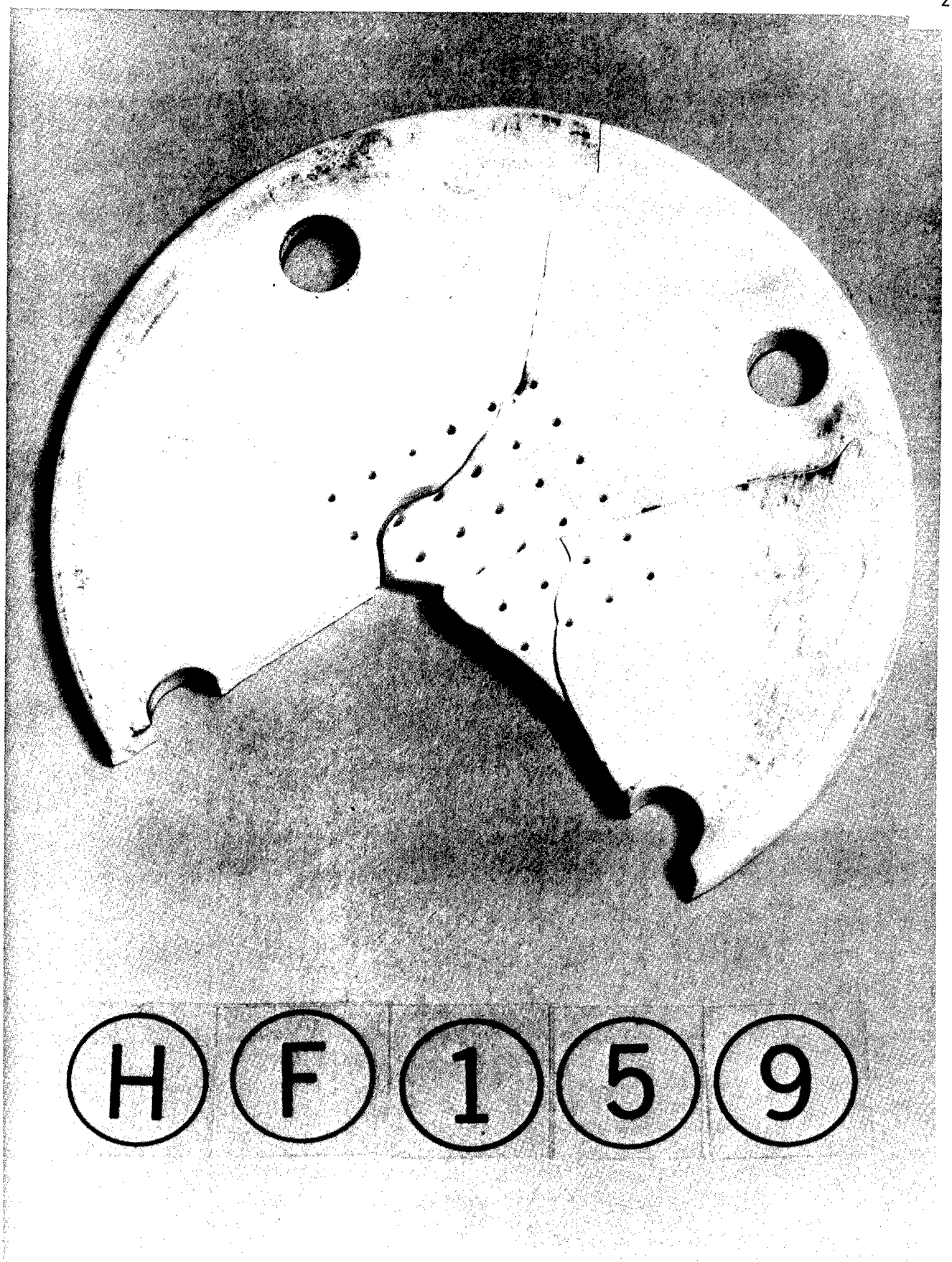

Figure 12. ALUMINA TEST PLATE — FACE EXPOSED TO HF FLAME.

A temperature versus time curve for run HF-171 is presented in Figure 13. According to the optical pyrometer readings, a "break point" occurs at 1738K, after which there is an additional temperature rise to 2041K. With this additional rise, other events had taken place during the run; the nickel specimen support and the tip of the thermocouple had melted, and the specimen had disappeared from view. The specimen, however, was recovered intact from the bottom of the test chamber.

B. Dense Calcium Hexaboride (CaB_6)

A dense sample of calcium hexaboride (CaB_6) was obtained with bulk density of 2.43 g/cm^3 and zero open porosity, representing 100% theoretical density. Previously, in run HF-87[2] CaB_6 with $\sim$ 21% porosity fragmented on initiation of the flame. With the dense specimen, however, a protective CaF_2 film formed, but some corrosion (i.e., Run 169, 4.5 wt % loss for $\sim$ 180 seconds of $\sim$ 1500K surface temperature) occurred. Additionally, CaB_6 is not as resistant to thermal shock as LaB_6, since CaB_6 specimens required programmed flame temperature increases, in $\leq$ 200K increments, above 1700K. Apparently, the fluoride (CaF_2) film affords some protection even above its melting point, up to the temperature where its viscosity becomes low enough to allow little substrate protection. Then, at T_f, as visually observed in run HF-167, the film was blown to the edge of the test cylinder, allowing rapid corrosion. A photograph of the specimen, tested in run HF-167, appears in Figure 14. Here the CaF_2 is seen as globules around the edge of the specimen and as a crescent-shaped layer (facing upward) on the top surface.

The temperature versus time curve for run HF-167 is presented in Figure 15. As indicated by the pyrometer readings, a "break point" occurs at 1661 K (1784K with emissivity correction) and there is an additional temperature rise to a maximum of 1924K.

C. Dense Yttria (Y_2O_3)

As with CaB_6, yttria (Y_2O_3) of high porosity ($\sim$ 38% open pores) fragmented upon exposure to the HF flame. Dense material was obtained with bulk density of 4.98 g/cm^3 and zero open porosity, representing 99% theoretical density. The material remained thermal shock sensitive but could be testing using programmed gas flows, allowing the measurement of T_f. From Table 1, it is apparent that film failure for Y_2O_3 is nearly identical to its fluoride (YF_3) melting point, implying that varorization or microcracking of the fluoride film have little effect on lowering its protection. The value of T_f = 1422K compares well to that for yttrium metal (1424K).

A temperature versus time curve for run HF-163, conducted with a dense Y_2O_3 specimen, is presented in Figure 16. As indicated, a "break point" occurs at 1340K (1422K with emissivity correction), and there is an

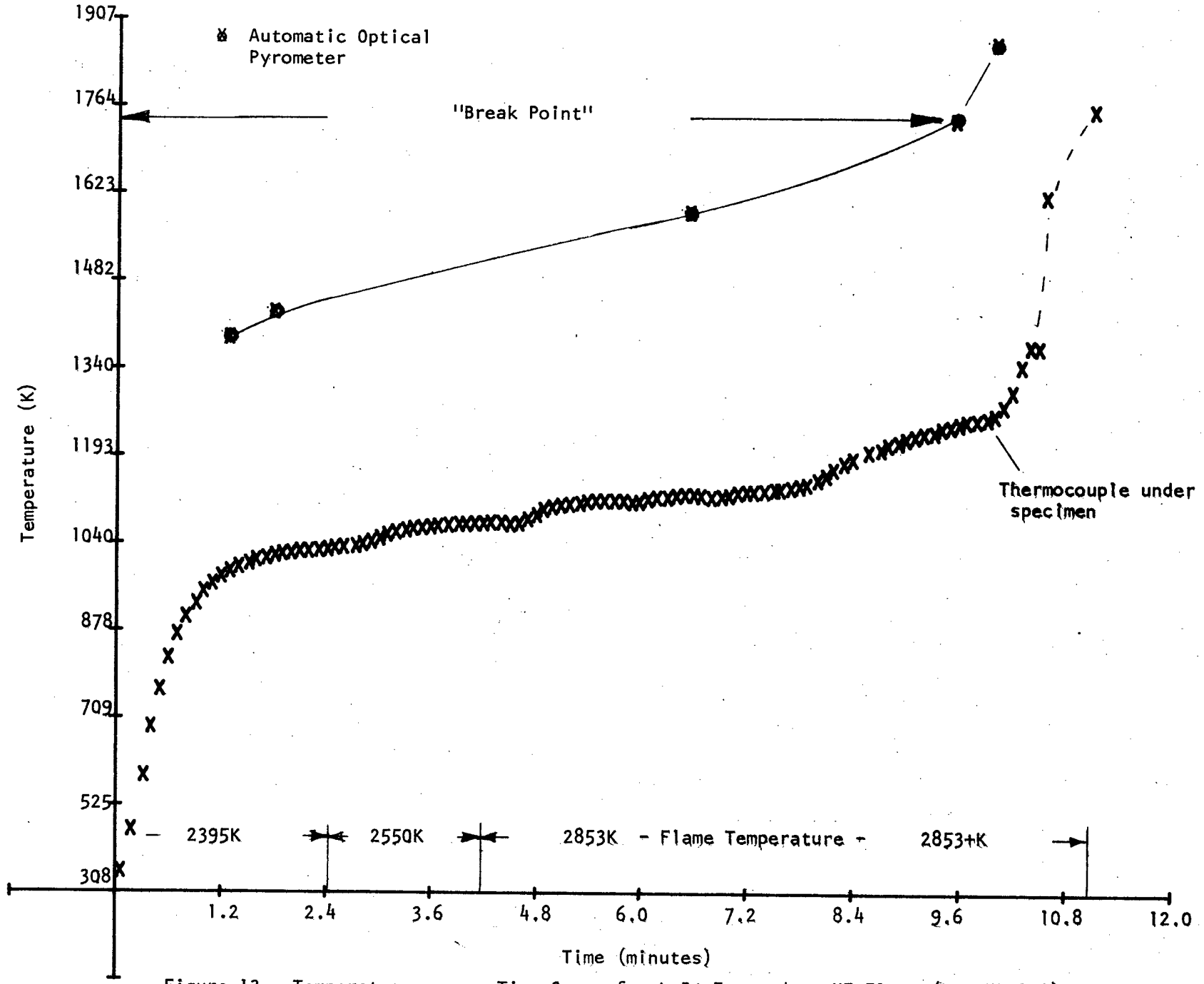

Figure 13. Temperature versus Time Curve for LaB_6 Exposed to HF Flame (Run HF-171).

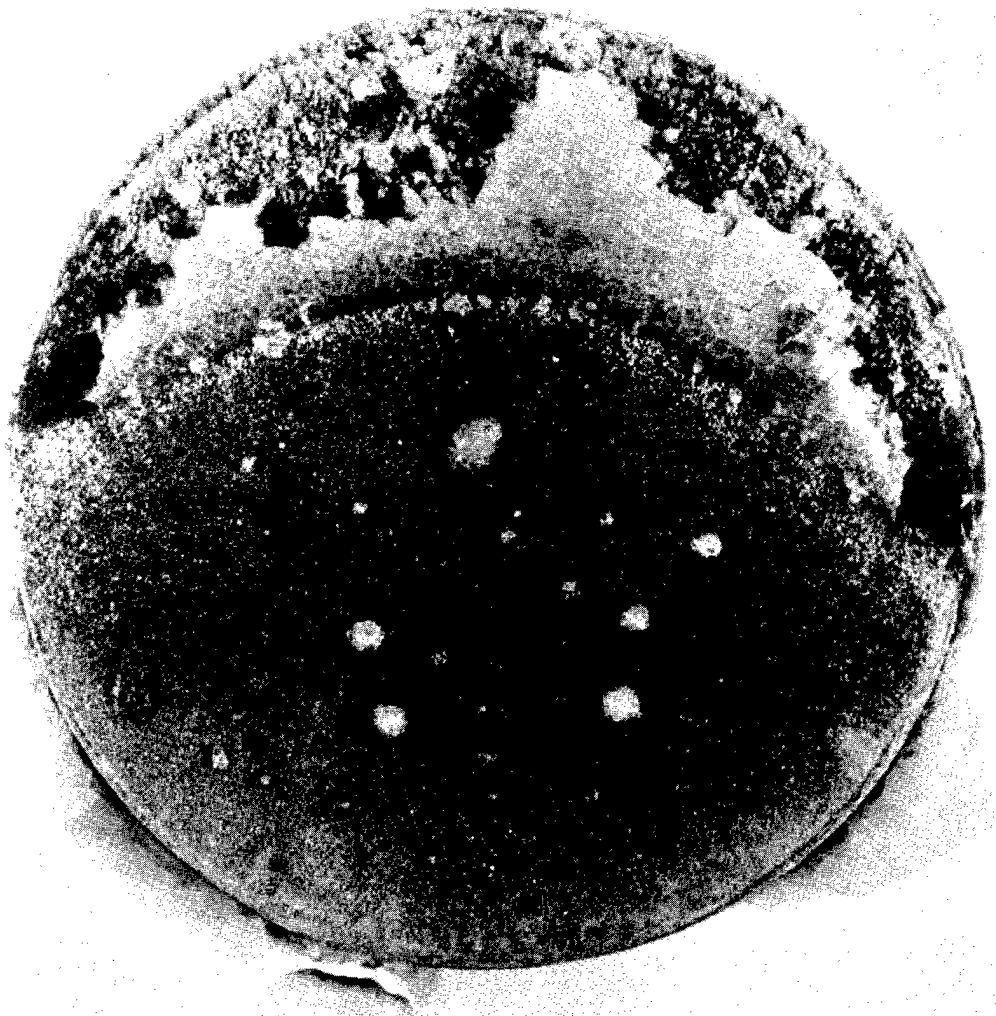

Figure 14. Calcium Hexaboride (CaB_6) Specimen Exposed to a HF Flame to a Temperature Exceeding the Maximum Surface Temperature for Near-Zero Corrosion - Run HF-167.

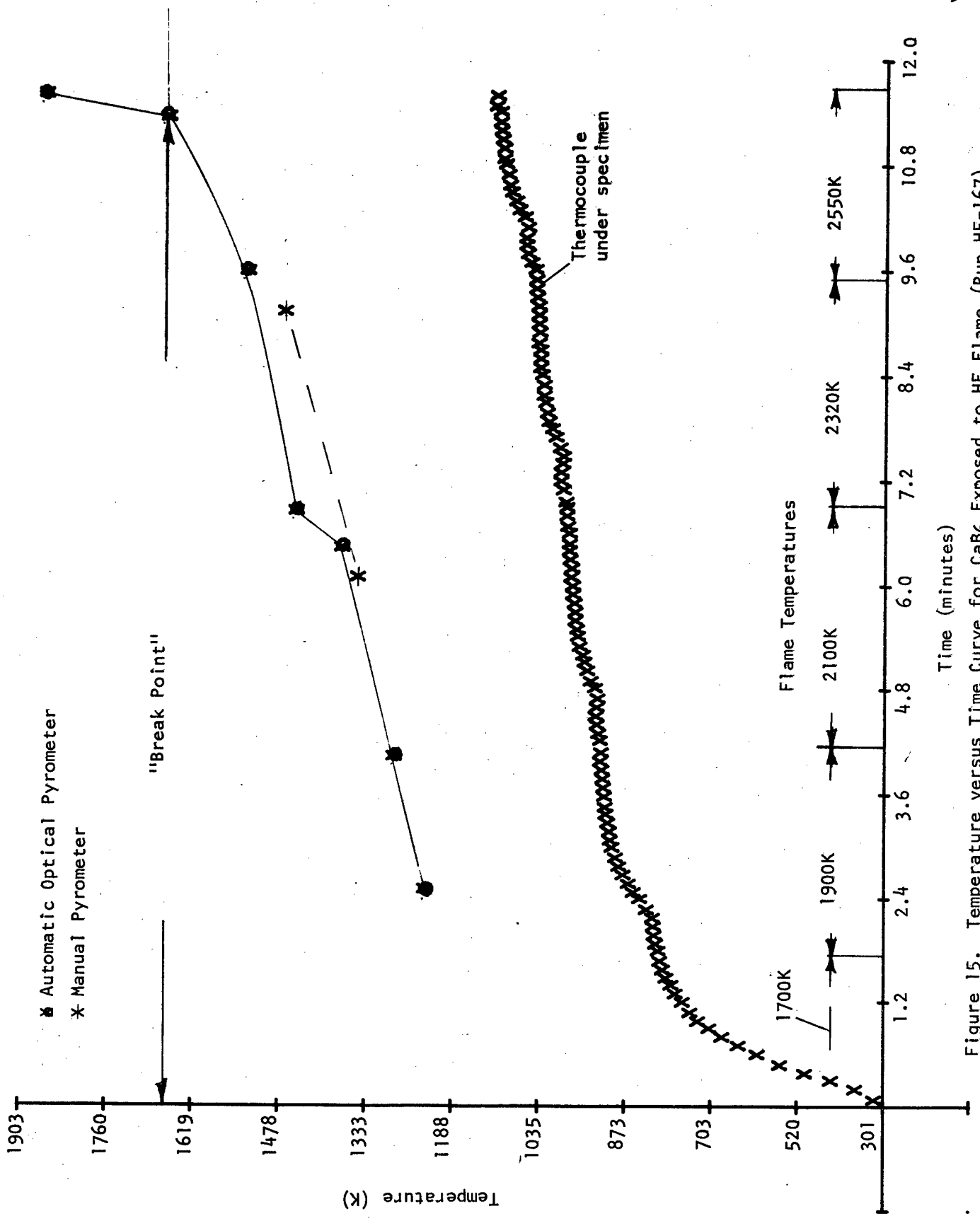

Figure 15. Temperature versus Time Curve for CaB_6 Exposed to HF Flame (Run HF-167).

Table 1

Material Performance in HF Environments

Material	Measured Fluoride Film Failure[1] Point (K)	Assumed Film Emissivity (ε)	Assumed Emissivity Correction[2] (K)	Fluoride Film Failure Point Including Emissivity Correction T_f (K)	Remarks[3]
SrO, HF-14	1375	0.4	86	1461	mp SrF_2 = 1740K
Y_2O_3, HF-163	1340	0.4	82	1422	mp YF_3 = 1420K
Graphite, HF-144	1138	-	-	1138	From top thermocouple
CaB_6, HF-167	1661	0.4	123	1784	mp CaF_2 = 1675K
LaB_6, HF-171	1738	0.4	136	1874	mp LaF_3 = 1765K

[1]Surface temperature above which rapid exothermic reaction occurs; unprotected by the fluoride film, a discontinuous jump in the surface temperature versus time profile enables ready definition of this point.

[2]From NBS Monograph 30.

[3]Melting points (mp) from B. Porter and E. A. Brown, J. Am. Ceramic Soc., 45, 49 (1962)

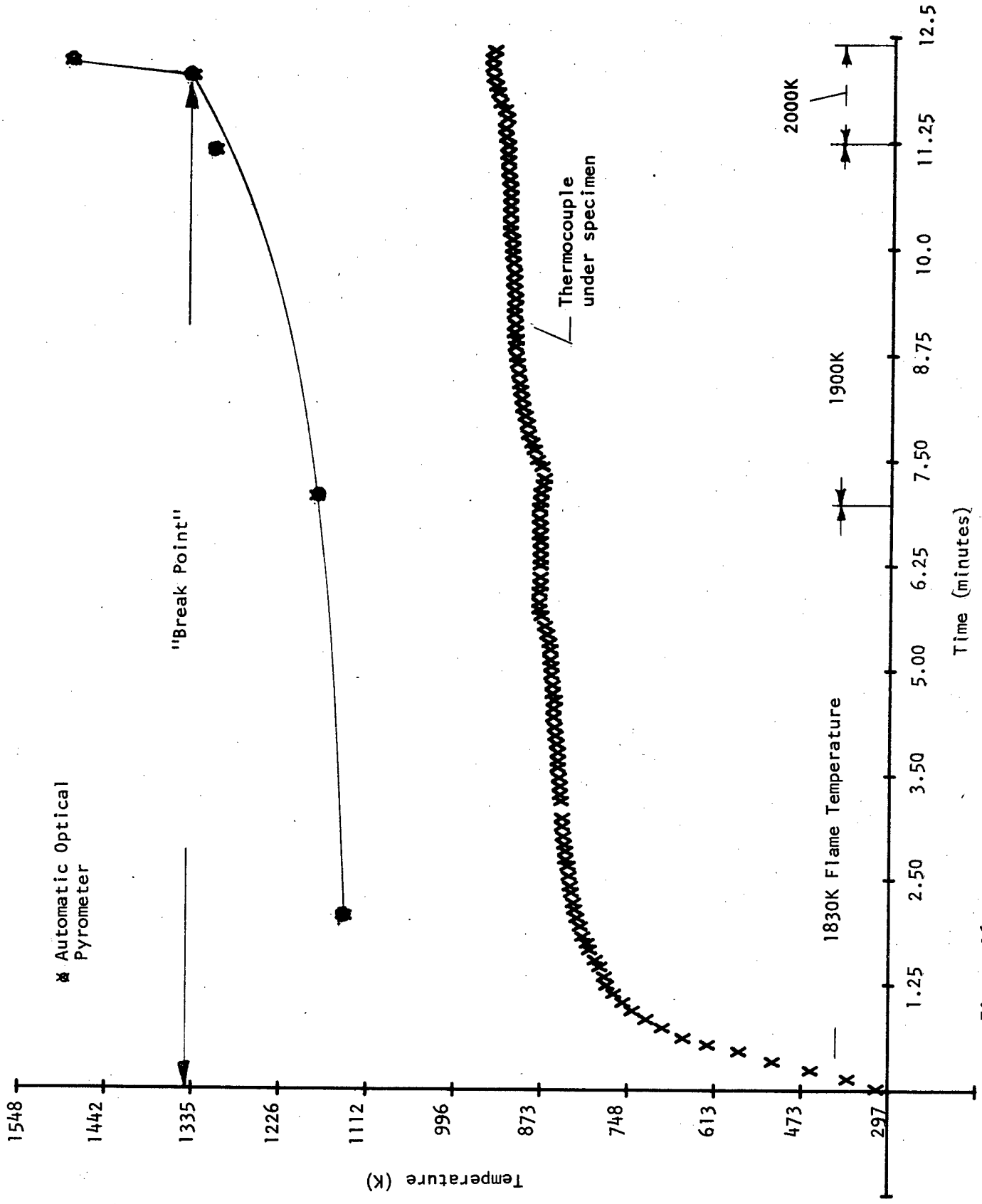

Figure 16. Temperature Versus Time Curve for Y_2O_3 Exposed to HF Flame (Run HF-163).

additional temperature rise to a maximum of 1486K. It might be mentioned that the specimen did break into three pieces after its temperature exceeded the "break point" temperature.

D. LaF_3/Ta Composite

A composite was considered combining the stable, high-melting lanthanum fluoride (LaF_3) with a ductile metal (Ta) that forms a volatile fluoride (TaF_5), with the prospect of reacting the Ta away on the surface; leaving the protective lanthanum fluoride. The mixture (15.3 wt % LaF_3 + 84.7 wt % Ta) was designed to have $\sim$ 33 vol % LaF_3. Two samples were prepared: one about 72% dense (9.3 g/cm^3 bulk density), isostatically pressed at 30 ksi and sintered at 1725K for 15 minutes in argon; the second, about 90% dense (from bulk dimensions and corrected for $\sim$ one-half of the LaF_3 content vaporizing) was hot pressed at 3.8 ksi for one hour at 1725K. Both specimens reacted vigorously with the HF flame, as demonstrated in runs HF-150, 151, and 152. The LaF_3 film was very poorly adherent and was quite porous. It is doubtful that a fully dense composite would have performed much better, since the large surface voids created throughout the LaF_3 film by the TaF_5 evaporation diminishes the protection.

E. Thermal Analyses

In order to better understand the relative protection afforded by fluoride films, the behavior of selected pure fluorides was studied by thermogravimetric analyses (TGA) and differential thermal analyses (DTA). The former technique yields information on the fluoride volatilization characteristics in vacuum ($< 1.3 \times 10^{-3}$ Pa), whereas the latter accurately defines melting points from heating and cooling curves. The data obtained are given in Table 2. Temperatures, Ti, represent weight loss initiation, whereas Te or T_3% represent the point where rapid weight losses occur, and indicate the upper use-temperatures of the pure fluorides in vacuum. These values are considerably lower than the fluoride film failure points (T_f) (see Table 1), determined for materials which form these fluorides; it is suspected that the excess fluorine ($2HF/F_2$) may suppress to some extent the fluoride volatilization in the torch environment.

Since there was a citation to an anomalous solid solution[13] at the $2SrF_2$-$1LaF_3$ composition, this mixture and the end members were examined by DTA. The SrF_2 and LaF_3 melting points are within 5K of reported values.[14] The $2SrF_2$-LaF_3 mixture melted 65K higher than LaF_3 and 95K higher than SrF_2; subsequent X-ray diffraction analyses revealed only the SrF_2 with a slightly shifted diffraction pattern indicative of the solid solution $2SrF_2$-$1LaF_3$ (since no LaF_3 was detected).

F. $La_{0.33}Sr_{0.67}B_6$ - Boride Solid Solution

Since the thermal analyses revealed the high melting point of the solid solution $2SrF_2$-$1LaF_3$, and since it has been reported[15] that a continuous solid solution of the borides LaB_6 and SrB_6 exists, the

Table 2

Fluoride Characterization by Thermal Analyses

Materials[2]	Characteristic Weight Change Temperatures[1] (K)[3]			Melting Points (K)[7]
	Ti[4]	Te[5]	$T_3\%$[6]	
AlF_3	900	995	980	-
CaF_2	1385	1590	1565	-
SrF_2	-	-	-	1740
LaF_3	1360	1640	1600	1770
$2SrF_2$-$1LaF_3$ Solid Solution	1435	1580	1575	1835

[1]Determined from TGA data using a Mettler Thermoanalyzer Model TA-1 with ultrahigh temperature (2773K) furnace using a vacuum < 1.33×10^{-3} Pa (< 10^{-5} torr), a heating rate of 10 K/min, and W/(W-26% Re) thermocouple, and with W crucibles

[2]Greater than 99.6 wt % pure by spark source mass spectrographic analyses

[3]Rounded to nearest 5K

[4]Initiation temperature as indicated by the initial change in slope of the weight loss curve

[5]Extrapolated temperature of rapid weight loss as determined by the intersection of tangent lines—one to the base curve and one to the point on the curve where 10% weight loss (based on initial weight) after 1273K occurred (or after 773K for AlF_3)

[6]Temperature at which 3% weight loss (based on initial weight) after 1273K occurred (or after 773K for AlF_3)

[7]Determined from DTA data using a Mettler Thermoanalyzer, Model TA-1 with high temperature (1873K) furnace, using a flowing (5.1 dm^3/hr) helium atmosphere, a heating rate of 8K/min, and Pt/(Pt-10Rh) thermocouple, and with Mo (Grade TZM) crucibles; average of four peaks

composition $La_{0.33}Sr_{0.67}B_6$ was prepared by reactive hot pressing the mixture (La_2O_3 + 4SrO + 8OB). About 25 wt % excess boron above the stoichiometric amount was used. Pressing at 2450K for three hours, under a pressure from 9.8 to 6.1 ksi, a specimen with a bulk density of 2.82 g/cm^3 and a theoretical density of 87% was obtained. The material was tested in run HF-161 and performed rather well, with some observed liquid formation on the surface of the specimen after having reached a maximum temperature of 1802K. Some internal fluoriding had occurred, and the fluoride coating was not very dense or adherent. Further testing of a dense specimen would be necessary to adequately compare the behavior of this hexaboride solid solution to LaB_6.

G. Plasma-Sprayed Lanthanum Hexaboride (LaB_6)

Since LaB_6 is a very high hardness material that requires either expensive diamond tool grinding or less familiar, nonconventional machining techniques (i.e., EDM, ECM, ECG), an improvement might be made in fabricating the compound by plasma spraying. Plasma-sprayed (P-S) material is $\sim$ 85-95% dense with flat grains that are not as strongly bonded as hot-pressed, more equiaxed grains. Thus, the P-S grains would "pull out" more readily by conventional machining, enabling the rapid shaping of relatively dense P-S layers (generally of 0.25 to 2.5 mm thickness). Additionally, P-S coatings can be used to provide protection for materials with less stringent performance requirements than, for example, nozzles. An instance would be the graphite test chamber assembly described in Section II.

By using -44, +25 μm size powder, it was possible to plasma spray LaB_6 successfully. Cylinders of nickel (coefficient of linear thermal expansion or CTE of 17.1 x 10^{-6}/K in the range 298-1273K), W-Ni-Fe (CTE of 5.2 x 10^{-6}/K), and POCO graphite (CTE of $\sim$ 7 x 10^{-6}/K) were plasma-spray coated with LaB_6 (CTE of 9.0 x 10^{-6}/K). The LaB_6 layers were all $\geq$ 0.18 mm (or $\geq$ 0.007 inch) and did provide a measure of protection for all substrates. However, cracking of the LaF_3 film layer occurred on shutdown for all but one POCO graphite specimen, which has a very close CTE match to the LaB_6. It is likely that by plasma-spraying mixed powders as an interlayer, an expansion gradient may be achieved (i.e., a Ni + LaB_6 interlayer on Ni followed by a pure LaB_6 layer). From the tests with different thicknesses of LaB_6 on POCO graphite, it appears, at this time, that a 0.71-mm (28-mil) coating will give the best protection. The LaB_6 coatings that were applied to the above test specimens were nonuniform in thickness. The uniformity of coatings may be a factor in the performance of a material, and an effort will be made to investigate this.

Three experiments were conducted with LaB_6 plasma-sprayed POCO graphite, namely, runs HF-153, 154, and 168. Runs HF-164 and HF-170, respectively, were conducted with a nickel-270 and a W-Ni-Fe-coated specimen. All data and results for these runs may be found in Appendices I and II.

The concept of plasma-spraying LaB_6 on materials to provide protection against $2F_2H_2$ environments will be explored further. It will be specifically applied to the testing of materials, as test plates, in the graphite test chamber assembly. In the fabrication of these test plates, experience will be gained in the machining of sprayed LaB_6 to prescribed dimensions. It is intended to fabricate a POCO graphite test chamber assembly sprayed with LaB_6, which should permit operation at temperature levels above which graphite would readily corrode.

SECTION IV. COMPILATION OF LANTHANUM HEXABORIDE DATA

A. Properties

In view of the fact that LaB_6 is generally unfamiliar to people in the materials field, a compilation of its properties is presented in Appendix III. Thermal diffusivity, thermal conductivity, and thermal expansion data on LaB_6, plotted as a function of temperature, are also presented along with comparison information on MgO, Al_2O_3, and BeO (see Figures 16, 17, and 18). In addition to the properties listed, LaB_6 is not water reactive and has excellent thermal shock properties.(3)

B. Machining Tests

Machining techniques which have been successfully used with borides are also mentioned in Appendix III. Of those cited, we, at the Y-12 Plant, have only tried diamond-tool cutting and drilling, and electrical discharge machining (EDM) to shape LaB_6 specimens.

Attempts to drill 40-mil-diameter holes ultrasonically in a specimen of LaB_6 were not satisfactory, in that the cores broke off in the drill resulting in drill breakage. Better success was obtained with a "precise" diamond-plated mandrel turned in a high-speed rotary grinding head at approximately 20,000 rpm; it took 3-5 minutes to drill a 150-mil-deep hole, 40 mils in diameter. In employing EDM techniques for drilling, it was found that it took 5-6 hours to drill a 60-mil-diameter hole, 1/4-inch deep.

An attempt to part a 1-inch-diameter LaB_6 cylinder in half with a plated diamond parting wheel took eight hours. Though not tried, it was felt that a resin-bonded diamond wheel would have given faster performance. The use of EDM to part a 1-inch-diameter cylinder also took eight hours; a copper/tungsten electrode was utilized in this instance. Here again, it was felt the job could have been done more quickly had a traveling wire electrode been employed.

Figure 16

THERMAL DIFFUSIVITY VERSUS TEMPERATURE FOR BeO, MgO, Al_2O_3, AND LaB_6

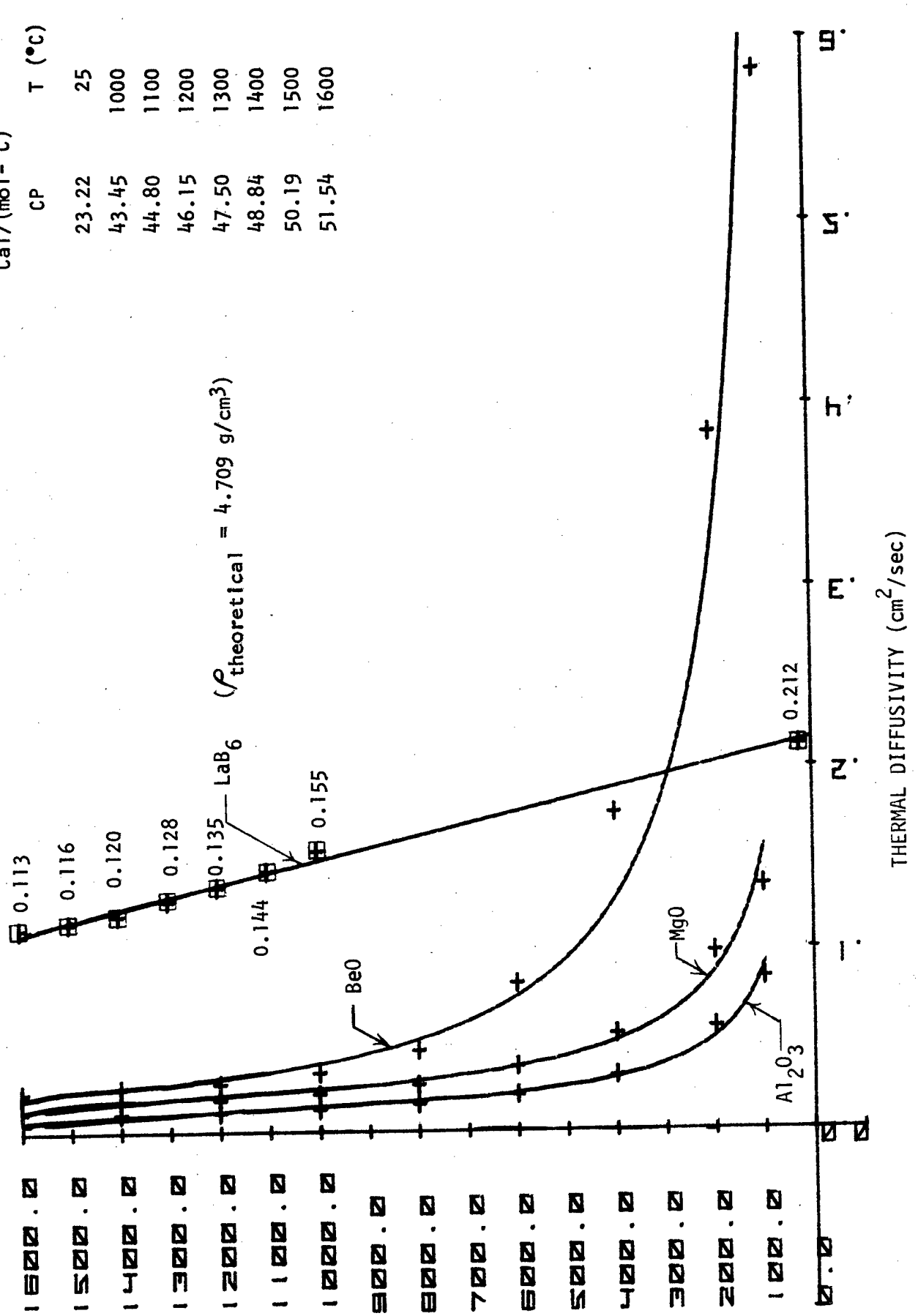

Figure 17

THERMAL CONDUCTIVITY VERSUS TEMPERATURE FOR BeO, MgO, Al_2O_3, AND LaB_6

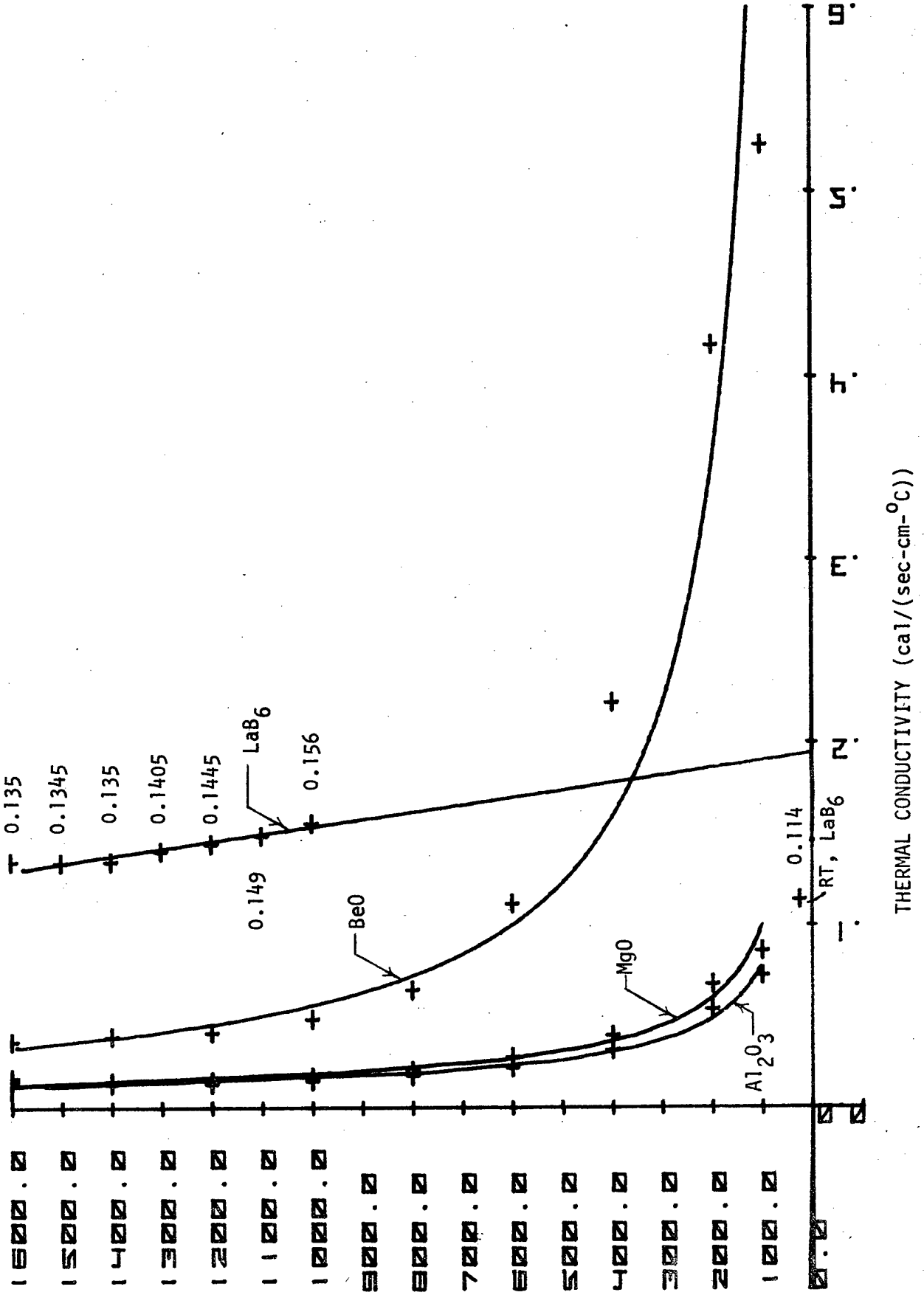

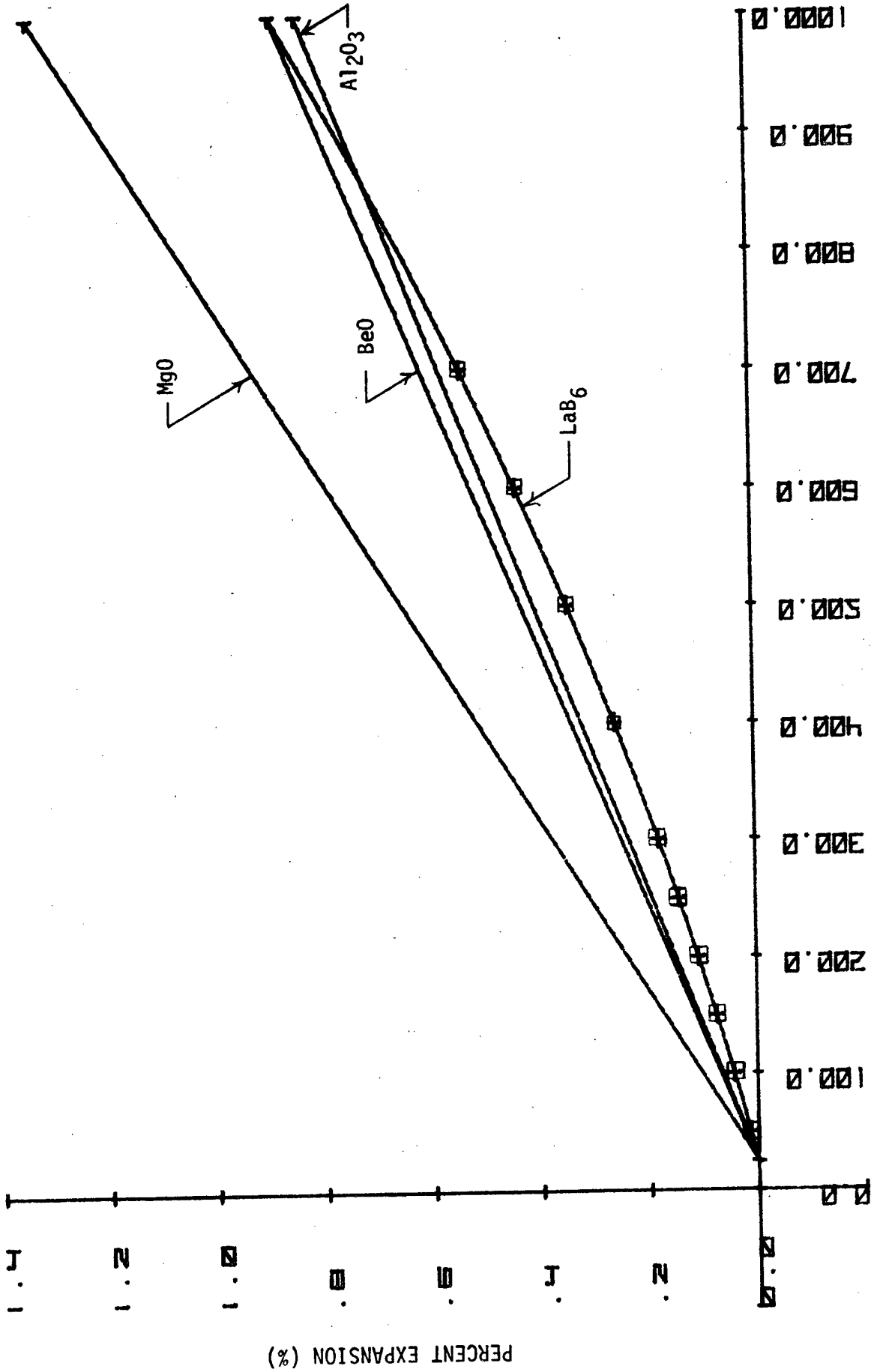

Figure 18

THERMAL EXPANSION VERSUS TEMPERATURE FOR BeO, MgO, Al_2O_3, AND LaB_6

CONCLUSIONS

Continued testing of materials behavior in hydrogen-fluorine environments has revealed:

1. As previously mentioned, material performance depends on the characteristics of its fluoride film. For substrate protection, the fluoride film must kinetically inhibit the fluoriding reaction. Fluoride film failure can occur by melting, vaporization, microcracking, or spalling.

2. A ranking of the best fluoride film formers with maximum use-temperatures for near-zero corrosion (or 95% T_f) in the range 1800-1400K is:

   LaB_6 > CaB_6 > $La_2O_3 \cdot Si_3N_4$ > (Sc, SrO, $LaCrO_3$, Ni)

3. Experiments conducted thus far with the graphite test chamber, in which test plate surface temperatures up to 1750K were attained, indicated little or no observable corrosion of the chamber body. Test plate data directly correlates with the data for test cylinders. Configuration was found to have an effect on the corrosion resistance of a specimen; i.e., the presence of sharp edges accelerates the initiation of corrosion.

4. Embedded thermocouple experiments do show temperature profiles for tested specimens.

5. A plasma-sprayed coating of LaB_6, nominally 0.7-mm thick, did provide protection for a POCO graphite substrate, when tested in the HF flame. The resultant LaF_3 layer was adherent and did not spall or crack upon cooldown after test.

REFERENCES

1. G. W. Weber, L. Kovach, C. E. Holcombe, and J. B. Condon, "Evaluation of Materials for Use in Hydrogen-Fluorine Environments," Report Y/DA-7321, Union Carbide Corporation, Nuclear Division, Oak Ridge Y-12 Plant, Oak Ridge, Tennessee; June 17, 1977.

2. C. E. Holcombe, L. Kovach, and G. W. Weber, "Materials for High-Temperature Hydrogen-Fluorine Environments," Report Y/DA-7477, Union Carbide Corporation, Nuclear Division, Oak Ridge Y-12 Plant, Oak Ridge, Tennessee; October 3, 1977.

3. C. E. Holcombe, L. Kovach, and G. W. Weber, "Materials for High-Temperature Hydrogen-Fluorine Environments," Report Y/DA-7745, Union Carbide Corporation, Nuclear Division, Oak Ridge Y-12 Plant, Oak Ridge, Tennessee; February 21, 1978.

4. G. V. Samsonov, High-Temperature Materials, No. 2, Properties Index, Plenum Press, New York; 1967, 418 pp.

5. G. V. Samsonov, High-Temperature Compounds of Rare Earth Metals with Consultants Bureau, New York, 1965, 280 pp.

6. S. N. L'vov, V. F. Nemchenko, and Yu. B. Paderno, "The Thermal Conductivity of Alkaline Earth and Rare Earth Metal Hexaborides," translation from Dokl. Akad. Nauk. SSSR, 149 (6), 353-4 (1963).

7. G. V. Samsonov, Yu. B. Paderno, and S. U. Kreingol'd, "Preparation of Lanthanum Hexaboride," J. Appl. Chem. of USSR (Russ. translation, Zhur. Prikl. Khim.), 34 (1), 8-13 (1961).

8. B. G. Arabei, E. N. Shtrom, and Yu. A. Lapitskii, "Characteristics of the Manufacturing Technology of Dense Parts from, and the Mechanical Properties of, Some Hexaborides of the Rare-Earth Metals," Powder Met. (Russ. trans., Poroshkovaya Met.), No. 5(23), 406-9 (1964).

9. N. N. Zhuravlev, A. A. Stepanova, Yu. B. Paderno, and G. V. Samsonov, "X-ray Determination of the Expansion Coefficients of Hexaborides," Russ. Cryst. (Russ. trans. Kristallografiya), 6 (5), 636-8 (1961).

10. N. N. Zhuravlev, I. A. Belousova, R. M. Manelis, and N. A. Belousova, "X-ray Determination of the Expansion Coefficients of Lanthanum and Yttrium Borides," Ibid., 15 (4), 723-4 (1970).

11. V. V. Fesenko and A. S. Bolgar, "Evaporation Rate and Vapor Pressure of Carbides, Silicides, Nitrides, and Borides," Powder Met. (Russ. trans., Poroshkovaya Met.), No. 1(13), 11-17 (1963).

12. J. M. Lafferty, "Boride Cathodes," J. Appl. Phys., 22 (3), 299-309 (1951).

13. H. J. Emeleus, "Nonvolatile Inorganic Fluorides", pp 1-76 (see page 44) in Fluorine Chemistry, Vol 1, edited by J. H. Simons, Academic Press, Inc., New York (1950).

14. B. Porter and E.A. Brown, "Melting Points of Inorganic Fluorides," J. Am. Ceram. Soc., 45(1), 49 (1962).

15. G. Blitznakov, I. Isolovski, and P. Pescher, Investigation on Cathode Materials Prepared from Mixed Metal Hexaborides," Rev. Int. Hautes Temp. Refract., 6(3), 159-64 (1969).

APPENDICES

APPENDIX I. SUMMARY OF TEST CONDITIONS DURING THE EXPOSURE OF SPECIMENS TO A HYDROGEN-FLUORINE FLAME

	Run No.															
	HF-138[a]			HF-139[a]		HF-140[a,d]	HF-141[d,a]					HF-142[d,a]				
Specimen Identification	MgO			ATJ Graphite		Nickel-270	LaB_6					LaB_6				
Source												HF-141				
Nozzle Flows, scfm																
Helium	3.8	3.6	3.3	3.7	3.7	3.0	3.6	3.0	2.6	2.45	3.6	3.6	2.6	2.1	2.1	3.6
Fluorine	0.9	1.0	1.4	1.0	1.1	1.6	1.0	1.6	1.7	1.9	1.0	1.0	1.7	2.0	2.0	1.0
Hydrogen	0.45	0.5	0.7	0.5	0.55	0.8	0.5	0.8	0.85	0.95	0.5	0.5	0.85	1.0	1.0725	0.5
	5.15	5.1	5.4	5.2	5.35	5.4	5.1	5.4	5.15	5.30	5.1	5.1	5.15	5.1	5.1725	5.1
Theoretical Flame Temperature, K	1700	1830	2215	1810	1900	2395	1830	2395	2550	2690	1830	1830	2550	2853	2853+	1830
Duration of Run, min	1	1	1.17	7	3.37	4.05	1	3.75	3.25	3.33	1.15	1	3.5	3.33	0.82	1.18
Thermocouple Reading under Specimen, °C			-	-	-	-										
Optical Pyrometer, °C			1010	-	1178	1384				1275					1423	
Thermocouple Experiment Readings, °C				(b)	(c)											
#1	-	-	881	752	1149	1425				1079					1270	
2			705	652	868	1000				998					1164	
3			830	740	1118	1425				1105					Failed[e]	
4			880	745	1136	1425				972	(slipped out of position)				1346	

(b) Before film left specimen
(c) After film left specimen
(d) Alumina grit under the specimen
(e) Nickel sheathing of the thermocouple melted

	Run No.																	
	HF-143(d)			HF-144(a)	HF-145(g)		HF-146(g)	HF-147(a)										
Specimen Identification		LaB_6						MgO - Single Crystal(f)										
Source				ATJ Graphite HF-139	ATJ Graphite Plate		ATJ Graphite Plate											
Nozzle Flows, scfm																		
Helium	2.6	2.1	2.6	3.7	3.6	3.8	3.7	3.8	3.6	3.7	3.6	3.45	3.3	3.6	3.7	3.6	3.8	
Fluorine	1.7	2.0	1.7	1.1	0.85	0.9	1.1	0.9	1.0	1.1	1.2	1.3	1.4	1.2	1.1	1.0	0.9	
Hydrogen	0.85	1.0	0.85	0.55	0.43	0.45	0.55	0.45	0.5	0.55	0.6	0.65	0.7	0.6	0.55	0.5	0.45	
	5.15	5.1	5.15	5.35	4.88	5.15	5.35	5.15	5.1	5.35	5.4	5.40	5.4	5.4	5.35	5.1	5.15	
Theoretical Flame Temperature, K	2550	2850	2550	1900	1700	1700	1900	1700	1830	1910	2000	2105	2215	2000	1910	1830	1700	
Duration of Run, min	2.33	3.17	1.23	3.1	3.17	2.43	7.42	3.25	1.67	2.0	1.5	2.75	1.75	1.17	1.0	1.0	1.0	
Thermocouple Reading under Specimen, °C		925		-	535		898											
Optical Pyrometer, °C		1240		1248	No indication		1440					1130						
Thermocouple Experiment Readings, °C																		
#1		-		1188	-		-				888	1070						
2		-		827	-		-				720	806						
3		-		1232	-		-				909	1097						
4		-		1132	-		-				750	865						

(f) Specimen had been previously exposed to a 1700K flame for 3.75 min and a 1830 K flame for 1.52 min; run was aborted because the flame was off-center; specimen developed cracks but did not fall apart.

	Run No.									
	HF-148[n]			HF-149[a]	HF-150[d]	HF-151			HF-152	
Specimen Identification	ATJ Graphite			NiAl	Ta-LaF_3[h]	Ta-LaF_3			Ta-LaF_3[k]	
Source						HF-150[j]				
Nozzle Flows, scfm										
Helium	3.6	3.3	3.6	3.1	3.8	3.6	3.7	3.6	3.3	3.8
Fluorine	1.0	1.4	1.0	1.5	0.9	1.0	1.1	1.2	1.4	0.9
Hydrogen	0.5	0.7	0.5	0.75	0.45	0.5	0.55	0.6	0.7	0.45
	5.1	5.4	5.1	5.35	5.15	5.1	5.35	5.4	5.4	5.15
Theoretical Flame Temperature, K	1830	2215	1830	2320	1700	1830	1910	2000	2215	1700
Duration of Run, min	2.0	1.58	1.42	3.25	3.1	2.67	1.58	2.05	1.03	5.12
Thermocouple Reading under Specimen, °C		1000		-	650	-	-	-	777	650
Optical Pyrometer, °C		∿ 1280		1350	1400				1545	1253
Thermocouple Experiment Readings, °C										
#1		-		1255	-				-	-
2		-		1004	-				-	-
3		-		1297	-				-	-
4		-		1208	-				-	-

(h) 33 vol % LaF_3; 67 vol % Ta

(j) White coating was brushed off leaving a black specimen with visible metallic flakes on surface

(k) Estimated density 90% of theoretical; LaF_3 may have left the mixture during fabrication of specimen

Run No.	HF-153									HF-154					HF-155 (g)	HF-156 (g)
Specimen Identification	POCO Graphite Sprayed with Nominal 7-mil coat of									POCO Graphite Sprayed with					MgO Plate	ATJ Graphite Plate
Source	LaB_6 (m)									Nominal 28-mil coat of LaB_6 (m)						
Nozzle Flows, scfm																
Helium	3.8	3.7	3.3	3.1	3.0	3.1	3.3	3.7	3.8	3.8	3.7	3.3	3.7	3.8	3.8	3.7
Fluorine	0.9	1.1	1.4	1.5	1.6	1.5	1.4	1.1	0.9	0.9	1.1	1.4	1.1	0.9	0.9	1.1
Hydrogen	0.45	0.55	0.7	0.75	0.8	0.75	0.7	0.55	0.45	0.45	0.55	0.7	0.55	0.45	0.45	0.55
	5.15	5.35	5.4	5.35	5.4	5.35	5.4	5.35	5.15	5.15	5.35	5.4	5.35	5.15	5.15	5.35
Theoretical Flame Temperature, K	1700	1900	2215	2320	2395	2320	2215	1900	1700	1700	1900	2215	1900	1700	1700	1900
Duration of Run, min	1.0	2.33	2.25	1.25	2.25	1.0	1.0	1.0	1.25	1.0	1.0	2.25	1.0	1.0	3.25	0.9	2.27
Thermocouple Reading under Specimen, °C					823							764				585	561
Optical Pyrometer, °C						1230						1235				∿ 1275	1327
Thermocouple Experiment Readings, °C					None							None				-	-
#1																	
2																	
3																	
4																	

(m) Top center of specimen had bump on it
(g) Chamber experiment
(a) Thermocouple experiment
(n) Flame calibration run

	Run No. HF-157[g]			HF-158[g]	HF-159[g]	HF-161		HF-162		HF-163		
Specimen Identification	Ni-200 Plate			ATJ Graphite Plate w/slots	Alumina Plate	SrB_6-LaB_6 Mixture		Y_2O_3		Y_2O_3		
Source								Ceradyne		Ceradyne		
Nozzle Flows, scfm												
Helium	3.8	3.7	3.45	3.8	3.8	3.3	3.1	3.8	3.6	3.6	3.7	3.6
Fluorine	0.9	1.1	1.3	0.9	0.9	1.4	1.5	0.9	1.0	1.0	1.1	1.2
Hydrogen	0.45	0.55	0.65	0.45	0.45	0.7	0.75	0.45	0.5	0.5	0.55	0.6
	5.15	5.35	5.40	5.15	5.15	5.4	5.35	5.15	5.1	5.1	5.35	5.4
Theoretical Flame Temperature, K	1700	1900	2105	1700	1700	2215	2320	1700	1830	1830	1900	2000
Duration of Run, min	3.0	2.08	3.32	6.25	5.65	3.5	3.82	3.33	1.88	7.0	4.25	1.18
Thermocouple Reading under Specimen, °C			772	595	580		840		617			676
Optical Pyrometer, °C			1137	1280	1117		1505		1268 976[p]			1193 1050[p]
Thermocouple Experiment Readings, °C			None	None	None		None		None		None	
#1												
2												
3												
4												

[p] Apparent "break point"

	Run No.												
	HF-164			HF-165				HF-166		HF-167			
Specimen Identification	Ni-270 Sprayed with LaB_6(t)			CaB_6				CaB_6		CaB_6			
Source				Ceradyne				Ceradyne		HF-165			
Nozzle Flows, scfm													
Helium	3.6	3.6	3.8	3.7	3.6	3.45	3.3	3.3	3.8	3.7	3.45	3.1	2.6
Fluorine	0.9	1.2	0.9	1.1	1.2	1.3	1.4	1.4	0.9	1.1	1.3	1.5	1.7
Hydrogen	0.45	0.6	0.45	0.55	0.6	0.65	0.7	0.7	0.45	0.55	0.65	0.75	0.85
	5.15	5.4	5.15	5.35	5.4	5.4	5.4	5.4	5.15	5.35	5.4	5.35	5.15
Theoretical Flame Temperature, K	1700	2000	1700	1900	2000	2100	2215	2215	1700	1900	2100	2320	2550
Duration of Run, min	2.67	4.6	3.0	2.25	2.25	1.25	3.58	34 sec	1.75				
Thermocouple Reading under Specimen, °C		723					774	-					840
Optical Pyrometer, °C		1160					1247	-					1620 1365(p)
Thermocouple Experiment Readings, °C	None			None				-					-
#1													
2													
3													
4													

(t) Nominal 18-mil coat

	Run No.														
	HF-168			HF-169					HF-170				HF-171		
Specimen Identification	POCO Graphite Sprayed with LaB_6[s]					CaB_6			W-Ni-Fe Sprayed with LaB_6[u]					LaB_6[r]	
Source						Ceradyne									
Nozzle Flows, scfm															
Helium	3.8	3.7	3.45	3.8	3.7	3.45	3.7	3.8	3.8	3.7	3.3	3.0	2.6	2.1	2.0
Fluorine	0.9	1.1	1.3	0.9	1.1	1.3	1.1	0.9	0.9	1.1	1.4	1.6	1.7	2.0	1.6
Hydrogen	0.45	0.55	0.65	0.45	0.55	0.65	0.55	0.45	0.45	0.55	0.7	0.8	0.85	1.0	1.0
	5.15	5.35	5.4	5.15	5.35	5.4	5.35	5.15	5.15	5.35	5.4	5.4	5.15	5.1	4.6[q]
Theoretical Flame Temperature, K	1700	1900	2100	1700	1900	2100	1900	1700	1700	1900	2215	2395	2550	2853	2853+
Duration of Run, min	2.17	2.0	3.0	1.42	1.83	3.75	1.17	1.0	1.92	2.33	4.18	2.42	1.75	6.83	
Thermocouple Reading under Specimen, °C			753			738					775			failed at 1341	
Optical Pyrometer, °C			1217			1233					1137				1730 1441[p]
Thermocouple Experiment Readings, °C			None			None					None			None	
#1															
2															
3															
4															

[q] Due to low F_2 supply pressure, F_2 flow had decreased near end of run

[r] Specimen rested on LaF_3 wafer and LaB_6 powder

[s] Nominal 14-mil coat

[u] Nominal 7-mil coat on top and 15-mil coat on the side

APPENDIX II. OBSERVATION ON TEST SPECIMENS EXPOSED TO A HYDROGEN-FLUORINE FLAME

Run No.	Material	Theoretical Flame Temperature (K)	Duration of Run (min)	Sample Surface Temperature (K)	Weight Loss (%)	Diameter Loss (%)	Height Loss (%)	Measured Loss in Height (mm)	Remarks
HF-138	MgO	1700	1						Thermcouple experiment specimen cracked vertically in plane passing through drilled thermocouple holes in about 3 minutes
		1830	1						
		2215	1.17	1299	0.02	0	0	0	
HF-139	ATJ Graphite	1810	7						Thermocouple experiment; specimen changed to a black velvet texture
		1900	3.37	1471	10.7	1.5	5.6	0.71	
HF-140	Ni-270	2395	4.05	1680	-	-	-	-	Thermcouple experiment; specimen melted; nickel-sheathed thermocouples fused to the specimen.
HF-141	LaB_6	1830	1						Thermocouple experiment. Top surface of specimen became grayish; bottom had a white coat
		2395	3.75						
		2550	3.25						
		2690	3.33	1571	0.16	+0.1	+0.1	+0.01	
		1830	1.15						
			12.48						
HF-142	LaB_6	1830	1						Thermocouple experiment specimen was gray on top with a white film on the bottom
	HF-141	2550	3.5						
		2853	3.33						
		2853+	0.82	1720	+0.12	0	0.4	0.05 (at center only)	
		1830	1.18						
			9.83						
HF-143	LaB_6	2550	2.33	1534	0.096	0	0	0	Specimen turned gray on top and had a white layer on the bottom
			3.17						
			1.23						
			6.73						

Run No.	Material	Theoretical Flame Temperature (K)	Duration of Run (min)	Sample Surface Temperature (K)	Weight Loss (%)	Diameter Loss (%)	Height Loss (%)	Measured Loss in Height (mm)	Remarks
HF-144	ATJ Graphite HF-139	1900	3.1	1543	8.1	0.8	5.9	0.7	Thermocouple experiment specimen corroded; two top thermocouple holes became visible
HF-145	ATJ Graphite	1700	5.6	No indication	+0.24	-	-	-	Test chamber run. There was a white coating on both sides of the test plate in area containing the holes. Rest of assembly appeared to be untouched
HF-146	ATJ Graphite	1900	7.42	1752	5.8	0	19.6 (max.)	0.76 (max.)	Test chamber run; area around holes in test plate corroded. Chamber assembly appeared to be untouched.
HF-147	MgO	1700	3.25						Thermocouple experiment. A portion of the specimen melted; corrosion was uneven. Center thermocouple hole became visible
	Single Crystal	1830	1.67						
		1910	2.0						
		2000	1.5						
		2105	2.75	1421	-	-	-	-	
		2215	1.75						
		2000	1.17						
		1910	1.0						
		1830	1.0						
		1700	1.0						
			17.09						
HF-148	ATJ Graphite	1830	2.0						Flame calibration run.
		2215	1.58	1576	10.9	1.6	4.4-6.6	0.84 (max.)	Specimen eroded
		1830	1.42						
			5.00						

Run No.	Material	Theoretical Flame Temperature (K)	Duration of Run (min)	Sample Surface Temperature (K)	Weight Loss (%)	Diameter Loss (%)	Height Loss (%)	Measured Loss in Height (mm)	Remarks
HF-149	NiAl	2320	3.25	1646	3.4[a]	0.97	1.5	0.2	Thermocouple experiment; the nickel-sheathed thermocouple and nickel specimen support reacted with the specimen. Bluish coloration on top of specimen.
HF-150	Ta-LaF_3	1700	3.1	1697	16.9	0.3	-	-	A white thick flaky nonadherent coating formed
HF-151	Ta-LaF_3	1830	2.67						White soft, nonadherent coating formed; some evidence of melting
	HF-150	1910	1.58						
		2000	2.05						
		2215	1.03	1845	37.9	-	-	-	
			7.33						
HF-152	$TaLaF_3$	1700	5.12	1548	19.9	+2.0/-1.0	+0.21	+0.03	White nonadherent coating formed
HF-153	Graphite sprayed	1700	1.0						White nonadherent coating formed
	with LaB_6	1900	2.33						
		2215	2.25						
		2320	1.25						
		2395	2.25						
		2320	1.0	1524	4.98	0.4	1.4	0.18	
		2215	1.0						
		1900	1.0						
		1700	1.25						
			13.33						
HF-154	Graphite sprayed	1700	1.00						White LaF_3 layer appeared to be adherent; bottom of specimen not having a LaB_6 coating reacted
	with LaB_6	1900	1.00						
		2215	2.25	1529	1.6	0	1.3	0.2	
		1900	1.0						
		1700	1.0						
			6.25						

Run No.	Material	Theoretical Flame Temperature (K)	Duration of Run (min)	Sample Surface Temperature (K)	Weight Loss (%)	Diameter Loss (%)	Height Loss (%)	Measured Loss in Height (mm)	Remarks
HF-155	MgO Plate	1700	3.25						Test chamber run; specimen cracked into several pieces. Holes in plate were enlarged
		1830	0.9						
			4.15	∿ 1583	+0.5	-	+0.7	-	
HF-156	ATJ Graphite Plate	1900	2.27	1635	0.97	0	9.9	0.38	Test chamber run. Slots were enlarged in test plate.
HF-157	Ni-200 Plate	1700	3.0						Test chamber run; slight corrosion around center of plate with an increase in some of the hole diameters
		1900	2.08						
		2105	3.32	1437	0.17	0	0.8	0.03	
HF-158	ATJ Graphite Plate	1700	6.25	1587	1.49	0	11.2	0.43	Test chamber run; slots became enlarged and corrosion had occurred, particularly in center of the plate
HF-159	Alumina Plate	1700	5.65	1416	-	-	-	-	Test chamber run; plate cracked and portion of it was lost. Some corrosion had occurred.
HF-161	SrB_6-LaB_6 Mixture	2215	3.5						Fluoride layer thick on top but porous; some indication of melting
		2320	2.82	1802	6.24	0.6	1.8	0.25	
			6.32						
HF-162	Y_2O_3	1700	3.33						Specimen split, melting occurred to weld the two pieces together
		1830	1.88	1563	+0.3	0	-3.0	0.28	
			5.21						
HF-163	Y_2O_3	1830	7.0						Specimen cracked into three pieces after "break point"
		1900	4.25						
		2000	1.18	1486	-	-	-	-	
			12.43	1340[a]					

[a] Apparent "break point" temperature

Run No.	Material	Theoretical Flame Temperature (K)	Duration of Run (min)	Sample Surface Temperature (K)	Weight Loss (%)	Diameter Loss (%)	Height Loss (%)	Measured Loss in Height (mm)	Remarks
HF-164	Ni-270 sprayed with LaB_6	1700	2.67						LaF_3 coating on side had cracks; coating on top separated
		2000	4.6	1452	0.16	+0.29	+0.19	+0.03	
			7.27						
HF-165	CaB_6	1700	3.0						Specimen had a white adherent film except in area of vertical support posts
		1900	2.25						
		2000	2.25						
		2100	1.25						
		2215	3.58	1542	6.1	0.2	0.8	0.08	
			12.33						
HF-166	CaB_6	2215	34 sec	-	-	-	-	-	Specimen broke into three pieces
HF-167	CaB_6	1700	1.75						Fluoride film had mostly melted off the top surface; some melt adhered to the side
	HF-165	1900	2.42						
		2100	2.75						
		2320	2.58						
		2550	2.2	1924	4.1	0.8	-7.5/+2.1	0.74	
			11.7	1661 [a]					
HF-168	POCO Graphite coated with LaB_6	1700	2.17						Fluoride layer cracked on top in a ring ~ 1/16 in from OD; probably occurred during cooldown
		1900	2.0						
		2100	3.0	1510	0.3	0.1	0.6	0.08	
			7.17						

Run No.	Material	Theoretical Flame Temperature (K)	Duration of Run (min)	Sample Surface Temperature (K)	Weight Loss (%)	Diameter Loss (%)	Height Loss (%)	Measured Loss in Height (mm)	Remarks
HF-169	CaB_6	1700	1.42						Specimen had white adherent coat on it except on bottom
		1900	1.83						
		2100	3.75	1527	4.5	2.0	0.8	0.08	
		1900	1.17						
		1700	1.0						
			9.17						
HF-170	W-Ni-Fe	1700	1.92						Top LaF_3 was cracked and was peeling off. Bottom may have reacted since it had not been sprayed
	sprayed with	1900	2.33						
	LaB_6	2215	4.18	1428	0.05	-0.1	0.2	0.03	
HF-171	LaB_6	2395	2.42						Droplets were seen before "break point" was recorded. Specimen support and thermocouple melted. No LaF_3 obvious on specimen. Specimen had metallic and copper-colored lumps on it
		2550	1.75						
		2853 }							
		2853+}	6.83	2041	9.2	2.2	3.3	0.46	
			11.0	1738[a]					

APPENDIX III

SUMMARY OF PHYSICAL-CHEMICAL PROPERTIES OF LaB_6 [4-11]

Property	Units	Temperature	Value	Comments
Formula Weight	g	-	203.78	
Color	-	-	-	Purple, metallic-like
Density	g/cm^3	298	4.709	By X-ray
Structure	-	-	-	Cubic, Space group Pm3m
Lattice Parameter	Å	298	4.1573±0.001	
Heat of Formation, $-\Delta H^\circ_{f,298}$	Kcal/mole	298	30.7	
Heat Capacity, Cp	cal/(mol-°K)	298	23.22	See Figure 16
Thermal Conductivity, κ	cal/(sec-cm-°K)	300	0.114±0.01	See Figure 17
Thermal Diffusivity, α	cm^2/sec	300	0.177	See Figure 16
Average Coefficient of Linear Thermal Expansion, $\bar{\alpha}$	K^{-1}	-	$6.4\pm0.5\times10^{-6}$ (293-1073 K)	By X-ray, see Figure 18
			$7.4\pm0.5\times10^{-6}$ (293-873 K)	By X-ray, see Figure 18
Melting Point	°K	-	2988	
Vapor Pressure of La over LaB_6	Pa	1993	9.07×10^{-3}	
Vapor Pressure of B over LaB_6	Pa	1993	4.97×10^{-3}	
Rate of Evaporation	$g/(cm^2\text{-sec})$	1993	1.54×10^{-6}	
Crystal Lattice Energy U	Kcal/mol	-	1770	
Debye Temperature, Θ	K	-	885	
Root-mean-square Amplitude of Thermal Vibrations of Atom Complexes, $\left(\bar{\mu}^2_{291}\right)^{1/2}$	Å	291	0.042	
Electrical Resistivity	Ω-cm	293	7×10^{-6}	
Thermal Coefficient of Electrical Resistance	K^{-1}		$+2.68\times10^{-3}$ (273-373 K)	

Property	Value	Temperature	Value	Comments
Coefficient of Thermal EMF	μV/K	-	7.0	
Electronic Work Function	eV	-	2.68	
Richardson Constant	Amps/(cm^2-K^2)	-	29	
Coefficient of Secondary Emission	-	-	0.95	
Hall Constant, R	cm^3/coulomb	-	-4.96×10^4	
Magnetic Susceptibility	mol^{-1}	-	60×10^{-6} (293-673K)	
Effective Magnetic Moment	Bohr magnetons	-	9.0	
Normal Spectral Emittance at λ=0.65 μm	-	-	0.82 (1073-1973 K)	
Microhardness	kg/mm^2	-	2065 (100-g load)	
Modulus of Elasticity	kg/mm^2 (msi)	-	41.0-48.8 (58.3-69.4)	Maximum values reported
Bending Strength, MOR	kg/mm^2 (ksi)	-	12.9-35.0 (19.3-49.8)	Maximum values reported
Reagent Resistance	-	293	-	Nearly insoluble in 1:1 (concentrated acid: H_2O dilution HCl, H_2SO_4, and 15% NaOH solution; completely soluble in 1:1 dilution HNO_3 or HNO_3 mixed with HCl or H_2SO_4.
Machining Techniques				1. Diamond-tool grinding, sawing, or polishing 2. Electrical discharge machining (EDM) 3. Electrical machining (ECM) 4. Electrochemical grinding (ECG) Electrolytes (for 3 and 4) suggested are 2.5N NH_4NO_3 or NH_4NO_3 mixed with Na_3PO_4

EXTERNAL DISTRIBUTION

SAMSO
Attention: Lt. Col. J. R. Doughty
Worldway Postal Center
Post Office Box 92960
Los Angeles, CA 90009

Rocket Propulsion Laboratory
Attention: Maj. John Dean
Edwards Air Force Base, CA

TRW/DSSG
Attention: Dr. Richard Ackerman
Dr. Joe Mace
Mail Station 01/2270
One Space Park
Redondo Beach, CA 90278

Rocketdyne
Attention: Dr. H. Carpenter
Dept. 590-175/B 833
M.C. BA0-4
6633 Canoga Park, CA 91304

Air Force Weapons Laboratory
Attention: Capt. N. Pchelkin
Capt. Paul Flynn
Maj. D. Olson
Kirtland Air Force Base, N. M. 87117

Air Force Materials Laboratory
Attention: Dr. H. Graham
Wright-Patterson Air Force Base, Ohio 45433

Los Alamos Scientific Laboratory
Attention: Dr. Roy Feber, CMB-8
Dr. Steven Stoddard, CMB-6
Dr. Terry Wallace, CMB-3
Dr. D. J. Sandstrom, CMB-6
Dr. P. Wagner, CMB-8
Los Alamos, New Mexico 87544

Bell Aerospace Company
Attention: Dr. Wayne Solomon
Dr. Frank Anthony
Post Office Box One
Buffalo, N. Y. 14240

Atlantic Research Corporation
Attention: J. R. MacPherson
5390 Cherokee Avenue
Alexandria, VA 22314

Yale University
Attention: Prof. Paul C. Nordine
Department of Engineering and Applied Science
Chemical Engineering Section
New Haven, CT 06520

U. S. Army Research Office
Post Office Box 12211
Research Triangle Park, North Carolina 27709

DARPA/Materials Sciences
Attention: Dr. Arden Bement
Capt. Harry Winsor
Dr. Stanley Ruby
1400 Wilson Blvd.
Arlington, VA 22209

Rice University
Department of Chemistry
Attention: Dean John L. Margrave
Post Office Box 1892
Houston, Texas 77001

United Technologies Research Center
Attention: Mr. Ronald Grose
Mr. Arthur Chalfante
East Hartford, Conn. 06108

Lawrence Livermore Laboratory
Attention: Dr. Don Olander
Post Office Box 808
Livermore, California 94550

Stanford Research Institute
Attention: Dr. D. L. Hildenbrand
333 Ravenswood Avenue
Menlow Park, CA 94025

U. S. Army Missile Research and Development Command
DRDMI-HAL
Attention: J. Walters
S. Clapp
Redstone Arsenal, AL 35809

INTERNAL DISTRIBUTION

H. D. Hickman
Z. L. Ardary
E. J. Barber, ORGDP
D. J. Bostock
J. M. Case
W. H. Dodson
R. L. Farrar, ORGDP
C. F. Hale, ORGDP
C. E. Holcombe
L. Kovach
G. B. Marrow
J. M. Mills, Jr./DOE-TIC
J. H. Pashley, ORGDP
L. R. Phillips
A. J. Taylor
W. H. Thompson, Jr./F. D. Bender
P. R. Vanstrum
W. J. Wilcox, Jr.
Y-12 Central Files (Y-12RC)